

Matematisk-fysiske Meddelelser  
udgivet af  
Det Kongelige Danske Videnskabernes Selskab  
Bind 33, nr. 14

---

Mat. Fys. Medd. Dan. Vid. Selsk. 33, no. 14 (1963)

---

RANGE CONCEPTS  
AND HEAVY ION RANGES  
(NOTES ON ATOMIC COLLISIONS, II)

BY

J. LINDHARD, M. SCHARFF(†) AND H. E. SCHIØTT



København 1963  
i kommission hos Ejnar Munksgaard

## CONTENTS

§ 1. Introduction . . . . .	Page
§ 2. Simple Unified Range Theory . . . . .	3
§ 3. Distribution in Range Measured along the Path . . . . .	4
§ 4. Projected Ranges and Associated Quantities . . . . .	17
§ 5. Comparison with Experiments . . . . .	24
References . . . . .	29
	40

## Synopsis

A theoretical discussion is given of the range of heavy ions with moderate velocity. The treatment is based on the theory of quasi-elastic collisions given elsewhere. The region where electronic and nuclear stopping compete is of particular interest. Use is made of a simple velocity proportional Thomas-Fermi type formula for electronic stopping, and a universal approximate differential cross section for scattering. Simplified models of nuclear scattering assuming power law scattering are also included. They turn out to be useful for exploratory computations of various range quantities.

The straightforward theory of ranges is studied in § 2. Range curves are computed for any atomic numbers of particle  $Z_1$ , and substance  $Z_2$ . It is found that when nuclear stopping is dominating, a  $\varrho - \varepsilon$  plot gives a universal range energy description.

Probability distribution in total range and various averages are studied (§ 3), in order to assess corrections to measurements when necessary. Similarly, corrections to measurements of projected ranges are obtained (§ 4). The range correction due to nuclear stopping is obtained for ions of high initial energy.

In § 5 a survey is given of numerous recent measurements of range. They are found to be in fair accord with theoretical results, for energies between 100 MeV (fission fragments) and  $\sim 1$  keV.

### § 1. Introduction

The present paper is a theoretical study of ranges of heavy ions of low velocity, and their connection to the basic problem of quasi-elastic collisions between ions and atoms. Three characteristic features give rise to complications. First, both electronic and nuclear stopping must be studied thoroughly, because they are similar in magnitude. Second, because of the frequent large deflections of the ions one must distinguish carefully between various range concepts. Third, the variety of choice of atomic number of both ion and substance gives an additional difficulty. We shall try to show that our present knowledge of quasi-elastic collisions, in spite of the above complications, can give us a simple and fairly accurate range theory. In point of fact, in the following we use a much simplified description of quasi-elastic collisions, which could be improved upon without difficulty. Aspects of quasi-elastic collisions are studied also in three associated papers: Notes on Atomic Collisions I, III, and IV. The aim is to exploit similarity properties of Thomas-Fermi type in collisions between heavy ions and atoms. In fact, similarity enables us to treat in a comprehensive way both slowing-down and damage effects by heavy ions.

The total range of a swift particle may be observed in track detectors like photographic emulsions. The observation of many tracks can then give the probability distribution in total range. In measurements of this kind the observed range depends on energy losses only, and not on scattering of the particle. For energetic heavy particles this separation of energy loss from scattering is especially valuable, since the two are due to unconnected processes, i. e. respectively electron excitation and Coulomb scattering by the atomic nuclei.

However, in nearly all other cases one observes somewhat different and less well-defined types of ranges. It is then customary to make corrections for multiple scattering in order to obtain the total range, but since these corrections are not insignificant—even in cases like high energy protons where deflections are small—it would seem appropriate to introduce explicitly these other types of ranges.

The scattering of a particle—in contrast to its energy loss—is always dominated by nuclear collisions, i. e. deflections in the screened electric field of the atom. In the case of electrons, large scattering angles are quite common during slowing-down. For heavy particles of high energy (e. g. protons with MeV-energies), scattering effects are relatively small, but since a high precision is desirable here, the distinction between different types of ranges again becomes important. Although the description in the following could be applied to electrons and to fast heavy particles, we shall aim at the case mentioned in the beginning of the introduction. In fact, for heavy ions of low velocity, e. g.  $v \sim v_0 = e^2/\hbar$ , scattering effects are large and the scattering can not be completely separated from energy loss, simply because the nuclear collisions here begin to dominate the energy loss too. This somewhat complicated case will be used as a basic example in our general discussion of range concepts.

The following discussion does not at all pretend to give an exhaustive treatment of range concepts. Thus, we are throughout concerned with stopping by a random system of atoms, i. e. uncorrelated atoms and separated collisions. This might never seem to include stopping of a relatively slow heavy ion in a solid, where the interatomic distance is short and atoms are arranged in a periodic lattice. Still, the effects are only sometimes large; they are not well understood and appear to be dependent on the structure of the lattice (cf. § 5).

Before turning to the various—and often complicated—range concepts and range distributions, we may take a more straightforward point of view. In § 2 we proceed as if the energy loss along the path was a nearly continuous process. This is not at all a poor first approximation. It both enables us to get a clearer picture of the essential points and permits comparisons with experiments (cf. § 5).

## § 2. Simple Unified Range Theory

Suppose that the range along the path is a well-defined quantity, so that we need not distinguish between e. g. average range, most probable range, and median range. We may introduce first the simple concept of specific energy loss,  $(dE/dR)$ ,—or average energy loss per unit path length—defined by

$$\frac{dE}{dR} = N \cdot S = N \int d\sigma T, \quad (2.1)$$

where  $N$  is the number of scattering centres (e. g. atoms) per unit volume and  $S$  the stopping cross section per scattering centre. Further,  $d\sigma$  is the differential cross section for an energy transfer  $T$  to atoms and atomic electrons.

The basic range concept is then obtained simply by integration of  $(dE/dR)$ ,

$$R(E) = \int_0^E \frac{dE'}{(dE'/dR)} = \frac{1}{N} \int_0^E \frac{dE'}{S(E')}. \quad (2.2)$$

The formulations (2.1) and (2.2) give a simple connection between range, specific energy loss, and differential cross section. We do not at present distinguish between different types of ranges. A better understanding of the connection between (2.2) and e. g. the average range is obtained in the detailed discussions in § 3.

In an analogous way we may introduce the range straggling (cf. BOHR (1948)). Similarly to (2.1) the average square fluctuation in energy loss becomes

$$\overline{(\Delta E)^2} = N \Omega^2 dR = NdR \int d\sigma T^2, \quad (2.3)$$

if the individual events have average occurrence  $NdRd\sigma$ , and are uncorrelated. We may next derive the average square fluctuation in range,  $(\Delta R)^2$ , using the present assumption that fluctuations are small,

$$(\Delta R)^2 = \int_0^E \frac{dE' N \Omega^2(E')}{(dE'/dR)^3} = \frac{1}{N^2} \int_0^E \frac{dE' \cdot \Omega^2(E')}{S^3(E')}. \quad (2.4)$$

If we were precise, we would say that the interpretation of (2.4) as the average square fluctuation in range is not quite correct. For the present purposes, however, we have by means of (2.2) and (2.4) defined the range,  $R$ , and its fluctuation,  $\Delta R$ , and the results are sufficiently accurate for most purposes. We now use (2.2) and (2.4) in a first study of the ranges of slow heavy ions.

Quite apart from using at first simple expressions like (2.2) and (2.4), it seems important—at the present stage of accuracy of theory and experiments—to be able to give a comprehensive description of slowing-down. It would for instance be futile to aim at an individual stopping curve for every one out of  $\sim 10^4$  possibilities for the set of atomic numbers ( $Z_1, Z_2$ ), where the suffixes 1 and 2 denote the penetrating particle and the atoms of the medium, respectively. If we are concerned with very high velocities, where the Bethe-Bloch stopping formula applies, the question of

dependence on  $Z_1$  drops out because the stopping is simply proportional to  $Z_1^2$ . In that case the dependence on  $Z_2$  is not far from being given by a Thomas-Fermi description, i. e. Bloch's relation  $I = Z_2 \cdot I_0$ , and only when high accuracy is demanded need we introduce deviations from the Thomas-Fermi results. Considering again the present case of comparatively low velocities, where the stopping is not proportional to  $Z_1^2$ , it is very important that descriptions of a Thomas-Fermi-like character are introduced, even though the resulting accuracy might not be high.

In point of fact, we hope to show in this section, and in § 5, that a Thomas-Fermi-like treatment of the dependence on both  $Z_1$  and  $Z_2$  has a quite satisfactory accuracy at the present stage of experimental precision. Our treatment should be based on a self-contained theory of the quasi-elastic collisions between ions and atoms. This theory will not be derived here; it is studied in two associated papers (Notes on Atomic Collisions, I and IV, unpublished). We shall merely summarize a few results of interest to us in the present connection (cf. also LINDHARD and SCHARFF, (1961)).

#### Electronic stopping

It is well known that for penetrating charged particles of high velocity, the energy loss to atomic electrons is completely dominating. The corresponding stopping cross section per atom is denoted by  $S_e$ , so that the specific energy loss is  $N \cdot S_e$ , where  $N$  is the number of atoms per unit volume. At high velocities  $S_e$  increases with decreasing particle velocity and has a maximum for a velocity of order of  $v_1 = v_0 \cdot Z_1^{2/3}$ . However, we shall consider low velocities only and in fact assume that  $0 < v < v_1$ . In the whole of this velocity region simple theoretical considerations lead to velocity proportional stopping, and a Thomas-Fermi picture shows that (Notes on Atomic Collisions, IV; see also LINDHARD and SCHARFF (1961))

$$S_e = \xi_e \cdot 8 \pi e^2 a_0 \cdot \frac{Z_1 Z_2}{Z} \cdot \frac{v}{v_0}, \quad v < v_1 = v_0 \cdot Z_1^{2/3}, \quad (2.5)$$

where the constant  $\xi_e$  is of order of  $Z_1^{1/6}$ , and  $Z^{2/3} = Z_1^{2/3} + Z_2^{2/3}$ . It is interesting that the approximate formula (2.5) holds down to extremely low velocities, i. e. also for  $v < v_0$ , in contrast to previous theoretical descriptions, where  $S_e$  was assumed to vanish for  $v \lesssim v_0$  (cf. BOHR (1948), SEITZ (1949)).

It should be emphasized that (2.5) is approximate in more than one sense. The constant in (2.5) is based on Thomas-Fermi arguments, and it is to be expected that fluctuations around this constant can occur, especially for  $Z_1 \gtrsim 10^*$ . Moreover, a precise proportionality to  $v$  will not be correct over the whole of the velocity region  $v < v_1$ . However, in the present context we shall not analyse electronic stopping in detail. As to stopping near the maximum  $v \sim v_1$ , cf. NORTHCCLIFFE (1963).

\* The presence of such ionic shell effects is confirmed in the systematic measurements by ORMROD and DUCKWORTH (1963), WIJNGAARDEN and DUCKWORTH (1962).

Another important circumstance may be mentioned. The energy loss to electrons is actually correlated to the nuclear collisions, and in close collisions considerable ionization will take place. Although the correlations are fairly well known, we disregard them in first approximation and consider electronic stopping as a continuous process. The correlation may be of some importance especially in straggling or higher order moments of the range.

#### Nuclear stopping and scattering cross section

A basic quantity is the nuclear stopping cross section,  $S_n$ . However, since the energy transfer in individual collisions can be quite large, the slowing-down by nuclear collisions cannot always be considered as a nearly continuous process. It is therefore important to know the differential cross section too. We shall here consider various approximations, of which the first one lends itself to a particularly simple mathematical treatment.

Suppose that there is a potential  $V(r)$  between the ion and the atom, such that  $V(r) = (Z_1 Z_2 e^2 a_s^{s-1} / s r^s)$ , with  $a_s \approx a = 0.8853 a_0 Z^{-1/3}$  (the number  $0.8853 = (9\pi^2)^{1/3} 2^{-7/3}$  is a familiar Thomas-Fermi constant). It is interesting that then the classical differential scattering cross section may be obtained approximately from an extrapolated perturbation procedure (Notes on Atomic Collisions I), leading to the simple result

$$d\sigma_n = \frac{C_n}{T_m^{1-1/s}} \frac{dT}{T^{1+1/s}}, \quad s \geq 1, \quad (2.6)$$

for an energy transfer  $T$  from the ion of energy  $E$  to an atom at rest. Here  $T \leq T_m = \gamma E = 4 M_1 M_2 (M_1 + M_2)^{-2} E$ ,  $T_m$  being the maximum energy transfer in the collisions. Furthermore, the constant  $C_n$  is connected to the stopping cross section  $S_n$ , and is approximately given by

$$C_n = \frac{\pi}{s} \left( b^2 \cdot a_s^{2s-2} \cdot \frac{3s-1}{8s^2} \right)^{1/s} \cdot T_m = \left( 1 - \frac{1}{s} \right) S_n, \quad (2.7)$$

where the collision diameter  $b$  is equal to  $2 Z_1 Z_2 e^2 / M_0 v^2$ ,  $M_0 = M_1 M_2 / (M_1 + M_2)$ . In the particular case of  $s = 1$ , i. e. simple Coulomb interaction, equation (2.6) also gives the correct Rutherford scattering, but in this case  $S_n$  in (2.7) does not represent the stopping cross section, the convergence of which is a result of adiabaticity in distant collisions.

As we shall demonstrate below, formulas of type of (2.6) are valuable for explorative purposes, interesting values of  $s$  being  $1, 3/2, 2, 3$  and  $4$ . The cross sections (2.6) are furthermore in accord with the Thomas-Fermi scaling of units. Corresponding to the case of  $s = 2$ , we shall sometimes approximate  $S_n$  by constant standard stopping cross section  $S_n^0$  (similar to that quoted by BOHR (1948)),

$$S_n^0 = (\pi^2 / 2.7183) e^2 a_0 Z_1 Z_2 M_1 \cdot Z^{-1/3} (M_1 + M_2)^{-1}. \quad (2.7')$$

Beside the simple power potential we study the case provided by a screened potential,  $U(r) = (Z_1 Z_2 e^2 / r) \cdot \varphi_0(r/a)$ , where  $\varphi_0$  is the Fermi function, and further

$a = a_0 \cdot 0.8853 (Z_1^{2/3} + Z_2^{2/3})^{-1/2}$ , which is a fair approximation to the ion-atom force. BOHR (1948) has employed a similar potential, with  $\exp(-r/a_B)$  in place of  $\varphi_0(r/a)$ ; however, an exponential function falls off too rapidly at large distances.

A screened Coulomb potential, involving only one screening parameter,  $a$ , leads for dimensional reasons to a natural measure of range and energy, for an ion colliding with atoms at rest. In fact, we may introduce, respectively,

$$\varrho = RNM_2 \cdot 4\pi a^2 \frac{M_1}{(M_1 + M_2)^2} \quad \text{and} \quad \varepsilon = E \frac{aM_2}{Z_1 Z_2 e^2 (M_1 + M_2)} \quad (2.8)$$

as dimensionless measures of range and energy. Note that  $\varepsilon^{-1}$  is essentially the parameter  $\zeta$  used by BOHR (1948). The scattering in the screened potential,  $U(r)$ , is obtained by means of the extrapolated perturbation method for classical scattering used in deriving (2.6), and one obtains a universal differential cross section

$$d\sigma = \pi a^2 \frac{dt}{2 t^{3/2}} f(t^{1/2}), \quad (2.9)$$

where  $t^{1/2} = e \cdot \sin(\theta/2)$  and  $\theta$  is the deflection in centre of gravity system. When elastic collisions are assumed, we find  $\sin^2(\theta/2) = (T/T_m)$ , where  $T$  and  $T_m$  are the energy transfer and its maximum value, respectively, in a collision with an atom at rest. The function  $f(t^{1/2})$  is shown in Fig. 1. At high values of  $t$  it approaches the Rutherford scattering. In Fig. 1 is also shown (2.6) for the case of  $s = 2$ .

It may be noted that the power law (2.6) leads to  $f = f_s$ , where

$$f_s(t^{1/2}) = \lambda_s \cdot t^{2 - \frac{1}{s}}, \quad 0.3 \lesssim \lambda_s \lesssim 1. \quad (2.6')$$

In the above, we have at first considered approximate potentials representing the ion-atom interaction and next, in an approximative way, derived the scattering from the potentials. However, we shall in the following take a simpler and more direct point of view. We consider (2.6) and (2.9) directly as approximations to the true scattering cross section and disregard the connection to a corresponding potential. This is the more justified, since the scattering is only quasi-elastic and cannot in detail be described by a potential between two heavy centres.

From (2.9) and Fig. 1 may be derived the nuclear stopping cross section, by means of the formula  $(de/d\varrho)_n = \int_0^\infty dx f(x) \varepsilon^{-1}$ . The result is shown in Fig. 2, together with the stopping from (2.6) for  $s = 2$ . Also the electronic stopping may be expressed in  $\varrho - \varepsilon$  units, and is then  $(de/d\varrho)_e = k \cdot \varepsilon^{1/2}$ , where the constant  $k$  varies only slowly with  $Z_1$  and  $Z_2$ , and according to (2.5) is given by

$$k = \xi_e \cdot \frac{0.0793 Z_1^{1/2} Z_2^{1/2} (A_1 + A_2)^{3/2}}{(Z_1^{2/3} + Z_2^{2/3})^{3/4} A_1^{3/2} A_2^{1/2}}, \quad \xi_e \approx Z_1^{1/6}. \quad (2.10)$$

Thus,  $k$  is normally of order of 0.1 to 0.2, and only in the exceptional case of  $Z_1 \ll Z_2$  can  $k$  become larger than unity. If  $Z_1 = Z_2$ ,  $A_1 = A_2$ , the constant  $k$  is given by the simple expression  $k = 0.133 Z_2^{2/3} A_2^{-1/2}$ . A representative case of electronic stop-

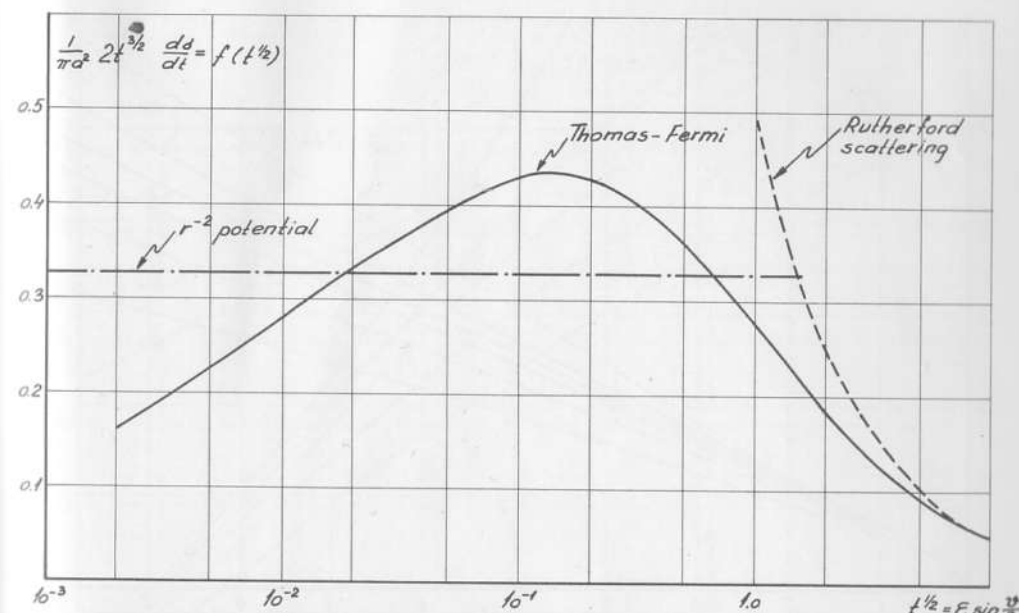


Fig. 1. Universal differential scattering cross section for elastic nuclear collisions, (2.9), based on a Thomas-Fermi type potential. At high values of  $t^{1/2}$  it joins smoothly the Rutherford scattering. The cross section corresponding to power law scattering (2.6), or (2.6'), with  $s = 2$  is also shown.

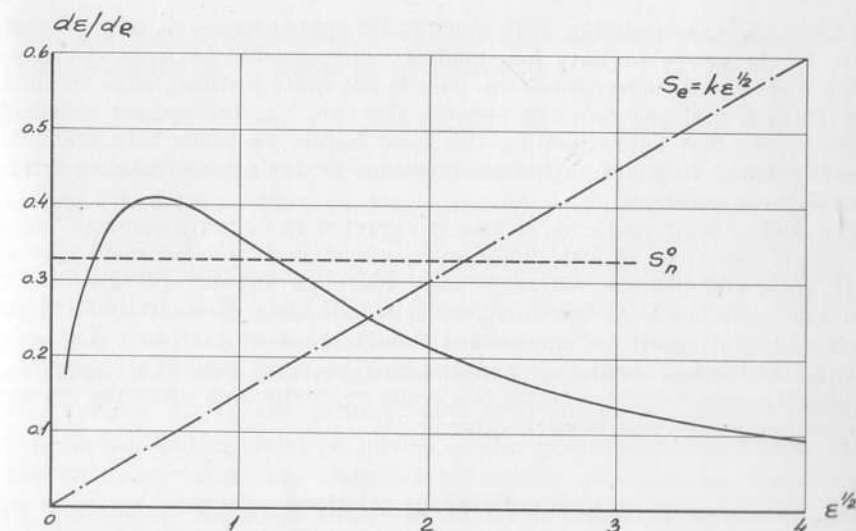


Fig. 2. Theoretical nuclear stopping cross section in  $\varrho - \varepsilon$  variables. The abscissa is  $\varepsilon^{1/2}$ , i.e. proportional to  $v$ . The full-drawn curve is  $(de/d\varrho)_n$ , computed from Fig. 1. The horizontal dashed line indicates (2.7). The dot-and-dash line is the electronic stopping cross section,  $k\varepsilon^{1/2}$ , for  $k = 0.15$ .

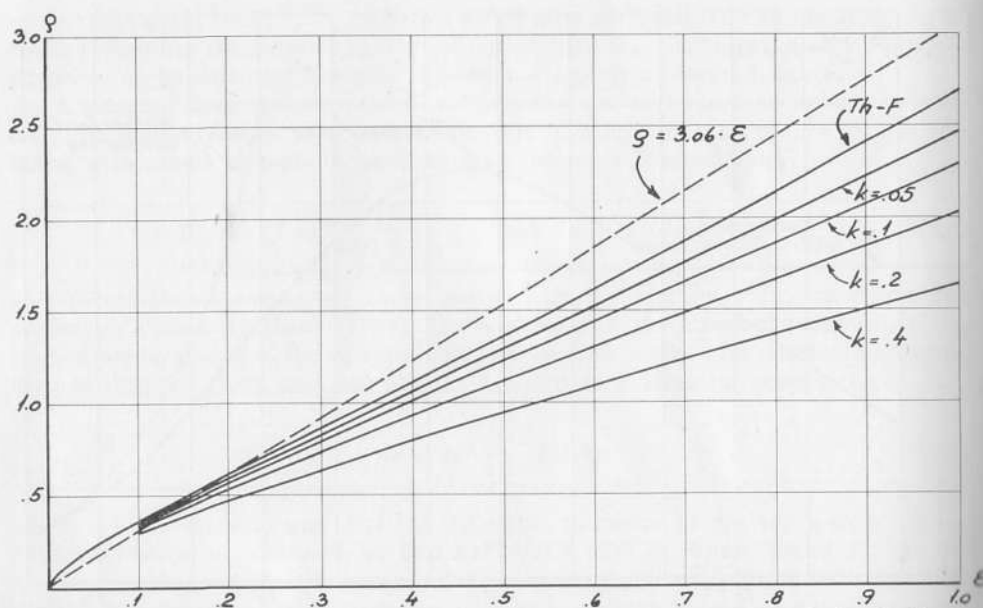


Fig. 3. Universal range-energy plot for  $\varepsilon < 1$ , cf. § 2 and § 3. The curve Th.-F. gives  $\bar{\rho}_1(\varepsilon)$ , i. e. (2.2), as a function of  $\varepsilon$  with neglect of electronic stopping. Curves for various values of the constant  $k$  in electronic stopping are also shown. Dotted straight line is the standard range,  $\rho = 3.06 \varepsilon$ .

ping,  $k = 0.15$ , is shown in Fig. 2. Formula (2.10) applies for  $v < v_1$ , or approximately  $\varepsilon < 10^3$ . In the above we have for simplicity distinguished between electronic excitation and elastic nuclear collisions. This is not quite justified, since in close collisions there is a strong coupling between the two, i. e. the nuclear collisions are not elastic. In first approximation this need hardly be taken into account; the reader is referred to Notes on Atomic Collisions IV for a more detailed treatment of quasi-elastic collisions.

The nuclear scattering cross section is expected to be fairly accurate, but while shell effects should be of little importance, a systematic overestimate may occur, due to neglect of inelastic effects. A more thorough discussion is given in Notes on Atomic Collisions I. At low energies nuclear stopping dominates over electronic stopping (2.5). It must be emphasized though, that at extremely low  $\varepsilon$ -values,  $\varepsilon \lesssim 10^{-2}$ , the nuclear scattering and stopping becomes somewhat uncertain, because the Thomas-Fermi treatment is a crude approximation when the ion and the atom do not come close to each other.

#### Range-energy relations

By means of the simple formula (2.2), and the above stopping cross sections, we are now able to estimate total ion ranges. Now, if we consider nuclear stopping only, and one screening length  $a$  in the scattering, the

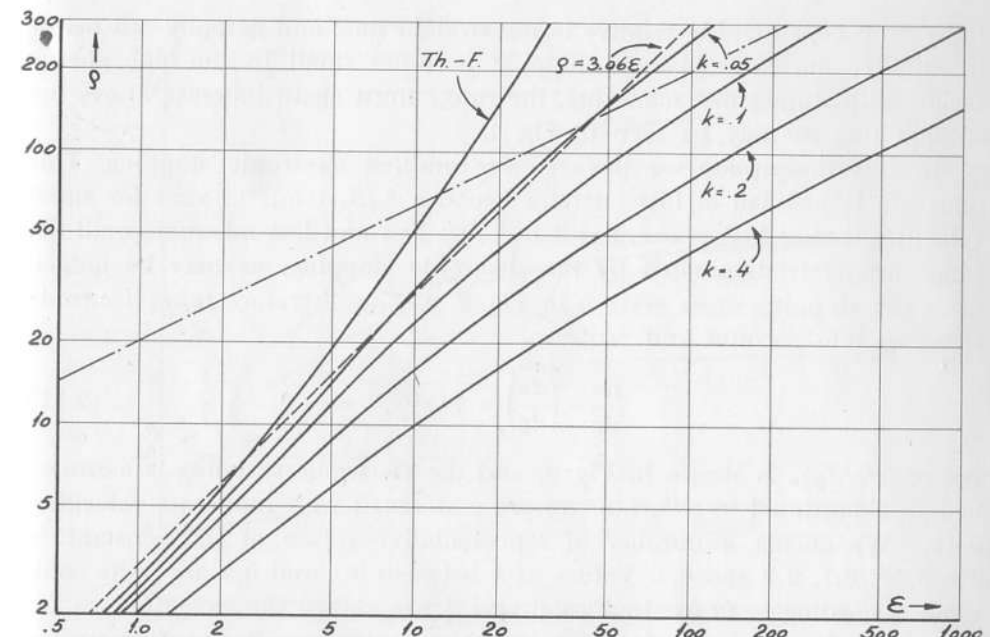


Fig. 4. The continuation at higher  $\varepsilon$ -values of the ranges  $\bar{\rho}_1(\varepsilon)$  in Fig. 3, for various values of constant  $k$  in electronic stopping. Straight dot-and-dash line is hypothetical range without nuclear stopping and  $k = 0.1$ .

dimensional arguments leading to (2.8) apply, and in these units the range in (2.2),  $\rho$ , must be a function of  $\varepsilon$  only, i. e.

$$\rho = \rho(\varepsilon)$$

for all ions and atoms. This formula holds both when (2.7) and when (2.9) is introduced in (2.2). The resulting range, based on (2.9) and  $f(t^{1/2})$  from Fig. 1 is shown by the solid curve in Fig. 3, for relatively small values of  $\varepsilon$ . The particular approximation of  $s = 2$ , i. e. the constant standard stopping cross section in (2.7') and Fig. 2 leads to the straight line  $\rho = 3.06 \varepsilon$  in Fig. 3. This standard range is closely similar to the range formula used by BOHR (1948) and also by NIELSEN (1956). For small  $\varepsilon$ -values the numerical curve remains above the straight line and has a downward curvature, corresponding to the effective power of the potential being higher than 2, in fact of order of 3. The detailed behaviour of the range curve can be easily understood from the stopping curves in Fig. 2. If we use the straight line as a standard in Fig. 3, i. e. the horizontal line as a standard in Fig. 2, the range must at first be higher than the standard straight line in Fig. 3. Next, since the actual stopping rises above the horizontal line, the range

must drop considerably relative to the straight line, and actually fall below it. Finally, since the nuclear stopping becomes small in the high energy region with Rutherford scattering, the range must again increase above the straight line as may be seen in Fig. 4.

In this description we have so far omitted electronic stopping. This omission is justified at low energies because  $(d\epsilon/d\varrho)_n$  tends to zero for small velocities, but at higher energies it becomes less and less adequate until the range finally is dominated by the electronic stopping, as may be judged from the stopping cross section in Fig. 2. Let us therefore take electronic stopping into account and write

$$\frac{d\epsilon}{d\varrho} = \left( \frac{d\epsilon}{d\varrho} \right)_n + k \cdot \epsilon^{1/2} \quad (2.11)$$

where  $(d\epsilon/d\varrho)_n$  is shown in Fig. 2, and the electronic stopping is assumed to be proportional to  $\epsilon^{1/2}$ , i. e. we are concerned with moderate velocities,  $v < v_1$ . We choose a number of representative values of the constant  $k$ ,  $k = 0.05, 0.1, 0.2$  and  $0.4$ . Values of  $k$  between 0.1 and 0.2 are quite common, according to (2.5). In Figs. 3 and 4 are shown the range curves for the above four values of  $k$ . The most conspicuous effects of electronic stopping are, first, that it leads to appreciable range corrections even at quite low  $\epsilon$ -values. Second, for  $\epsilon$  large compared to unity, the reduction in range always dominates, so that the range never increases above the straight line  $\varrho = 3.06 \epsilon$ , in contrast to the range with neglect of electronic stopping. In Fig. 4 is also shown the hypothetical range  $\varrho = (2/k) \epsilon^{1/2}$ , which would result if there were no nuclear stopping, in the case of  $k = 0.1$ .

By means of curves like those in Figs. 3 and 4 we are able to compare or estimate ranges for all ions in all substances but only for  $\epsilon$ -values below, say,  $\epsilon = 10$  are curves for the various  $k$ -values fairly close together and easy to compare. For light ions in heavy substances deviations start at even smaller  $\epsilon$ -values, because  $k$  becomes quite large. Moreover, only for these low values are we able to check in a direct manner the nuclear stopping, which here remains dominating.

Although we may well use Fig. 4 for estimates of ranges when  $\epsilon \gg 10$ , we can in this case introduce a more critical comparison between theory and experiments. In fact, it is apparent from Fig. 2 that for high values of  $\epsilon$  the range is mainly determined by the electronic stopping, and only a minor range correction is due to nuclear stopping which dominates at low values of  $\epsilon$ . Since nuclear stopping drops off quickly while electronic stopping increases, the nuclear stopping correction to the range remains fairly con-

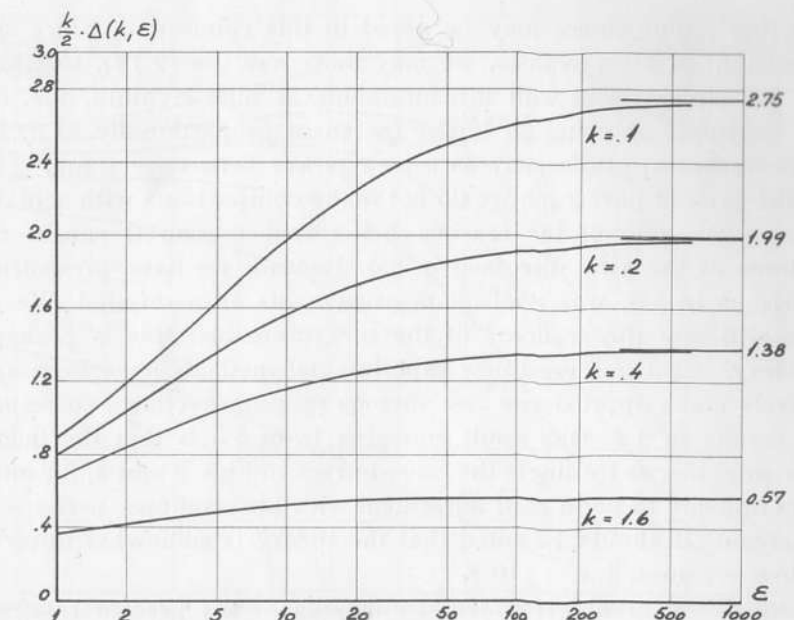


Fig. 5. Range corrections for nuclear stopping,  $(k/2) \Delta(k, \epsilon)$ , from equ. (2.12). Curves are shown for  $k = 0.1, 0.2, 0.4$  and  $1.6$ . Asymptotic values are roughly  $\Delta \rightarrow 1.76 \cdot k^{-3/2}$ .

stant above a certain value of  $\epsilon$ . We then introduce an extrapolated electronic range

$$\begin{aligned} \varrho_e(\epsilon) &= \int_0^\epsilon \frac{d\epsilon'}{(d\epsilon'/d\varrho)_e} = \int_0^\epsilon \frac{d\epsilon'}{(d\epsilon'/d\varrho)} + \int_0^\epsilon \frac{(d\epsilon'/d\varrho)_n \cdot d\epsilon'}{(d\epsilon'/d\varrho) \cdot (d\epsilon'/d\varrho)_e} \\ &= \varrho(\epsilon) + \Delta(k, \epsilon). \end{aligned} \quad (2.12)$$

The quantity  $\Delta(k, \epsilon)$  can be computed from the above formulas, and adding  $\Delta$  to an observed  $\varrho(\epsilon)$ , we obtain the extrapolated electronic range, which in our case of  $v < v_1$  should be equal to  $\varrho_e = (2/k) \epsilon^{1/2}$  (cf. dot-and-dash line in Fig. 4).

The function  $\Delta(k, \epsilon)$  is shown in Fig. 5 for  $k$ -values between 0.1 and 1.6. This procedure is probably the most direct way of comparing theoretical predictions of electronic stopping like (2.5) with range observations. The point is here that  $\Delta$  often is a relatively small correction, and in estimating the range correction  $\Delta$  we may use (2.5), even if this formula be not too accurate. Examples of the application of (2.12) and Fig. 5 are shown in § 5, cf. Figs. 14 and 15.

Another circumstance may be noted in this connection. Since  $\Delta$  tends to a constant at high  $\varepsilon$ -values, we may moreover use (2.12), together with Fig. 5, for comparisons with measurements at high  $\varepsilon$ -values, i. e.  $v >> v_1$ , where electronic stopping no longer increases proportionally to  $v$ , but instead decreases approximately as  $v$  to a power between -1 and -2.

In the present paragraph we do not make comparisons with actual range measurements, one of the reasons being that measured ranges require corrections of the kind discussed in § 4. Instead, we have presented these comparisons in § 5, where recent measurements are compiled. We do not discuss critically the accuracy of the measurements; this is perhaps unsatisfactory, because several new experimental methods have been applied. We merely make approximate and obvious range corrections, corresponding to the results in § 4. One result emerging from § 5 is that the theoretical nuclear stopping, as leading to the range curves in Figs. 3 and 4, for moderate  $\varepsilon$ -values appears to be in good agreement with observations, perhaps within  $\sim 20$  percent. It should be noted that the theory is somewhat uncertain at quite low  $\varepsilon$ -values, i. e.  $\varepsilon \lesssim 10^{-2}$ .

Beside the general experimental checking of the present range-energy relations there are several other ways of comparison. An immediate possibility is to measure directly stopping powers, which has been done in a few cases, but mostly when electronic stopping dominates. We shall not enter more critically into these questions, since the theory of electronic stopping is not the topic of the present paper. Nor will we attempt a detailed discussion of individual inelastic collisions between energetic ions and atoms at rest. But it may be mentioned that more subtle comparisons of ranges may be made. For instance, isotope effects are quite informative, and can elucidate both electronic and nuclear stopping, cf. § 5.

#### Range straggling

The simple description used here, with a range along the particle path based on (2.2), may now be extended to include an average square fluctuation in range, given by (2.4). This description contains the assumption that range fluctuations are relatively small. We may suppose that the fluctuations around the average correspond nearly to a Gaussian. In fact, if this were not so, the distribution in range would have a sizable skewness. Then we would have to distinguish between e. g. the most probable and the average range, and the simple relation (2.2) would have to be revised. Still, even in such cases the results in the present paragraph may be useful. We can in fact consider the present ranges, i. e. (2.2) as an approximation to the

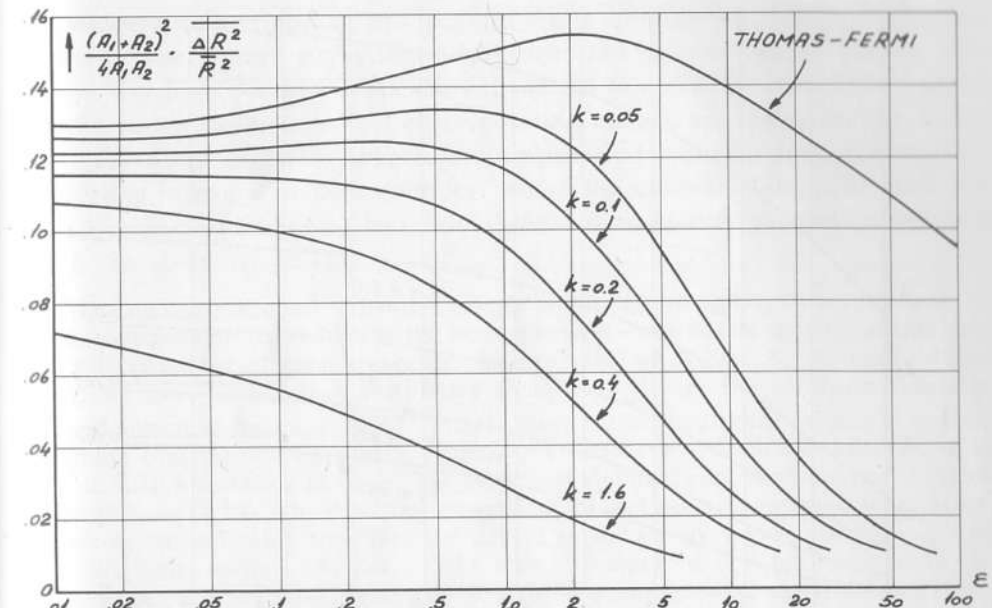


Fig. 6. Relative square straggling in range  $(\Delta R^2)_1/R_1^2$ , divided by  $\gamma = 4 M_1 M_2/(M_1 + M_2)^2$ . Curves are shown for several values of constant  $k$  in electronic stopping.

average range, and similarly consider the present range fluctuation, i. e. (2.4), as an approximation to the average square fluctuation in range. These averages are defined irrespective of the skewness of the distribution; they are studied in more detail in § 3, where also the accuracy of the present treatment is discussed more closely.

It is convenient to consider the relative square straggling in range,  $(\Delta\varrho/\varrho)^2 = (\Delta R)^2/R^2$ . Consider first nuclear stopping only, and in particular the power potentials represented by (2.6). Then we easily find

$$\left(\frac{\Delta\varrho}{\varrho}\right)^2 = \frac{s-1}{s(2s-1)} \gamma, \quad (2.13)$$

where  $\gamma = 4 M_1 M_2/(M_1 + M_2)^2$ . We thus obtain the extremely simple result that the relative straggling is independent of the range itself. It is moreover interesting to note that the result (2.13) is rather insensitive to  $s$  in the neighbourhood of  $s = 2$ . When  $s$  increases from 2 to 3 the relative square straggling decreases by only 20 percent. Thus the simple model predicts that at low energies  $(\Delta\varrho/\varrho)^2$  should be of order of  $\gamma/6$  (cf. also LINDHARD and SCHARFF (1961), LEACHMAN and ATTERLING (1957), HARVEY (1960)). We have here

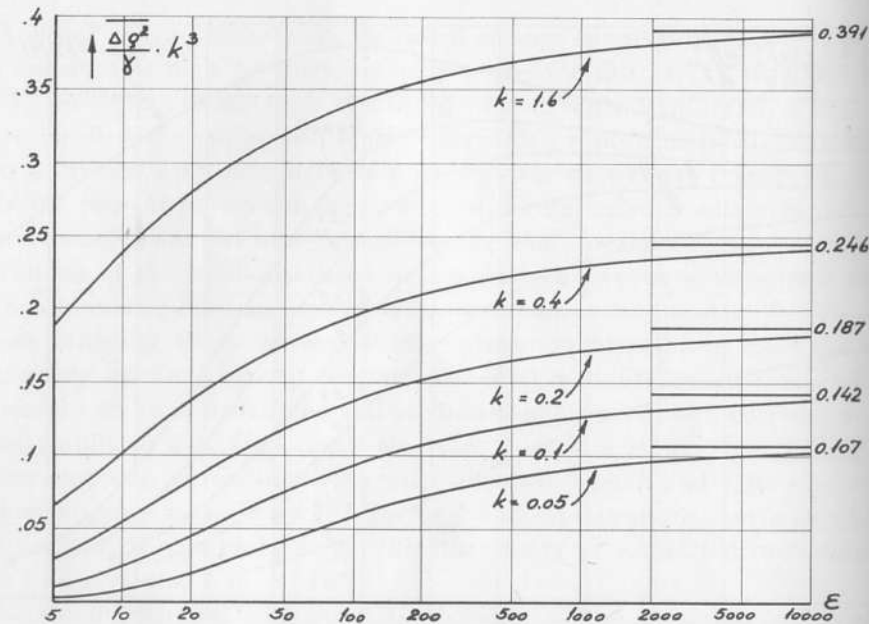


Fig. 7. Absolute straggling in range  $(\Delta\varrho/\varrho)^2$ , at high values of  $\varepsilon$ . Saturation values of the straggling are indicated.

considered the application of (2.6) to the simple formulas (2.2) and (2.4). A more detailed study of the probability distribution in range is made in § 3, on the basis of the power law scattering (2.6). It is shown there that the right hand side of (2.13) is only the first term in a power series expansion in  $\gamma$ .

We next apply the numerical Thomas-Fermi-type cross section (2.9) for scattering in nuclear collisions. We do this at first with neglect of electronic stopping, and by means of (2.4) we compute  $(\Delta\varrho/\varrho)^2 \cdot \gamma^{-1}$  against  $\varepsilon$ , as shown by the upper curve in Fig. 6. The relative straggling is seen to behave as expected from the simple power potential. Next, we include electronic stopping, using (2.5) and assuming that the contribution to straggling from electronic stopping is negligible\*. Clearly, it must lead to a reduced relative straggling. The results are shown in Fig. 6, for  $k = 0.05, 0.1, 0.2, 0.4$  and  $1.6$ . At  $\varepsilon$ -values around 1 to 10 a considerable reduction in the relative straggling sets in. The reduction corresponds to the circumstance that in this

\* This assumption can be questioned, since quasi-elastic collisions imply a correlation between the two types of energy loss, i. e. nuclear and electronic stopping. The assumption requires that a considerable part of electronic stopping occurs at impact parameters where recoil of the atom is small or moderate.

region electronic stopping has become quite dominating, and the absolute value of the square straggling,  $(\Delta\varrho)^2$ , does not increase much beyond this point. For high  $\varepsilon$ -values it is then convenient to consider the absolute value of the range straggling. The corresponding curves are given in Fig. 7, for various values of  $k$ . We therefore conclude that accurate measurements of straggling in range at high energies, where the electronic stopping does not at all correspond to (2.5), may give information about the predicted values of  $k$ , as given by (2.10).

The above treatment of simple ranges and range straggling is intended to be fairly comprehensive, and from the accompanying curves it is easy to obtain reasonable estimates of these quantities for any value of  $Z_1, A_1, Z_2, A_2$  and  $v$ . However, we have disregarded completely those cases where the substance contains several atomic elements,  $Z_2^{(1)}, Z_2^{(2)}, \dots$ , in given ratios. In all such cases, the nuclear stopping contribution from each element may be derived from the solid curve in Fig. 2, with a rescaling of units. The electronic stopping contributions are obtained from (2.5) or (2.10). The resulting ranges can be derived by numerical integration. However, considerable simplification occurs in an energy region where, e. g. the stopping cross section  $S^{(i)}$ , due to any atomic component  $i$ , is proportional to the same power of  $E$ , because in this case straightforward computations of averages may be made. For two components,  $a$  and  $b$ , we have  $R = R_a R_b (R_b x_a + R_a (1 - x_a))^{-1}$ , where  $R_a$  and  $R_b$  are the ranges in  $a$  and  $b$ , and  $x_a$  and  $1 - x_a$  are the relative abundances of  $a$  and  $b$ . Similar procedures may be used in the case of straggling in range.

### § 3. Distribution in Range Measured Along the Path

In the present chapter we shall try to go one step beyond the treatment in § 2, where only a simple range straggling was considered, and where it was tacitly assumed that straggling effects were small. We wish to check the validity of this picture and also to extend it. A basic reason for the extended treatment are the large fluctuations, known to result from encounters between slow heavy ions and atoms. We therefore attempt to study the probability distribution in range measured along the path. Although this distribution is much simpler than the distribution in space of the endpoint of the path, it is not easily obtained. One might perhaps employ Monte Carlo methods\* for the solution of representative cases, but we shall limit the treatment to typical and simple approximations, and in particular consider the power law scattering cross sections given by (2.6).

Consider again a particle  $(Z_1, A_1)$  with energy  $E$ , in a medium  $(Z_2, A_2)$ .

\* Monte Carlo methods were applied by e. g. ROBINSON, HOLMES and OEN (1962) to various models of nuclear scattering, but with neglect of electronic stopping, cf. also HOLMES (1962).

We denote by  $R$  the range measured along the particle path, i. e. the total distance traversed by the particle. Let  $p(R, E) dR$  represent the probability that the particle has a range between  $R$  and  $R+dR$ , so that

$$\int_0^\infty p(E, R) dR = 1 \quad \text{and} \quad \langle R^m \rangle = \int_0^\infty p(E, R) R^m dR.$$

An integral equation for  $p(E, R)$  may be derived as follows. Suppose that the particle with energy  $E$  moves a path length  $\delta R$  in a medium containing  $N$  atoms per unit volume. There is then a probability  $N\delta R d\sigma_{n,e}$  for a collision specified by energy transfer  $\sum_i T_{ei}$  to electrons (electrons labelled by suffix  $i$ ) and by an energy transfer  $T_n$  to translational motion of the struck atom. The particle will thus have an energy  $E - T_n - \sum_i T_{ei}$ . If the collision takes place, the particle has a probability  $p(R - \delta R, E - T_n - \sum_i T_{ei})$  of obtaining the total range  $R$ . Multiplying by the probability of collision,  $N\delta R d\sigma_{n,e}$ , we get the contribution from this specified collision to the total probability for range  $R$ . We next sum over all collisions. There is left a probability  $1 - N\delta R \int d\sigma_{n,e}$  that no collision occurs. In this event we clearly get a contribution  $(1 - N\delta R \int d\sigma_{n,e}) \cdot p(R - \delta R, E)$  to the total probability for the range  $R$ .

Collecting the above contributions we have an alternative expression for  $p(R, E)$ ,

$$p(R, E) = N\delta R \int d\sigma_{n,e} p(R - \delta R, E - T_n - \sum_i T_{ei}) + (1 - N\delta R \int d\sigma_{n,e}) \cdot p(R - \delta R, E),$$

and in the limit of  $\delta R \rightarrow 0$ ,

$$\frac{\partial p(R, E)}{\partial R} = N \int d\sigma_{n,e} \left\{ p(R, E - T_n - \sum_i T_{ei}) - p(R, E) \right\}, \quad (3.1)$$

which expression constitutes the basic integral equation governing the probability distribution in range along the path. In the remainder of this chapter we study the integral equation (3.1) and its consequences, using a number of approximations. We shall not further elaborate on the derivation of (3.1), but it may be noted that the formal limit of  $\delta R \rightarrow 0$  corresponds to separability between consecutive collisions. If there is no separability, the equation still holds, or may be easily amended, as long as collisions with moderate or large  $T$ -values remain separable.

Besides separability we have assumed that successive collisions are not correlated. This holds if the atoms in the substance are in fact randomly distributed, or if e. g. impact parameters corresponding to sizable deflections are extremely small compared to interatomic distances, giving effectively uncorrelated events. A system where collisions are separated and uncorrelated may be termed a random system of atoms. The derivation of (3.1) is based on a random system, and we limit our treatment to this case. A solid with periodic lattice is for many purposes a random system, but at low ion energies deviations from (3.1) can occur. These deviations contain directional effects and are sensitive to lattice structure, cf. p. 32.

On the assumption that energy losses to electrons are small and separated from nuclear collisions, we obtain

$$\left. \begin{aligned} \frac{\partial p(R, E)}{\partial R} &= N \int d\sigma_n \left\{ p(R, E - T_n) - p(R, E) \right\} \\ &\quad - NS_e(E) \frac{\partial}{\partial E} p(R, E), \end{aligned} \right\} \quad (3.2)$$

which formula is somewhat less general, but applicable to our previous cross sections for scattering.

We may rewrite (3.2) on the assumption that the Thomas-Fermi-like scattering formula (2.9) applies (note that this also includes (2.6) and (2.6')), and then introduce the variables  $\varrho$  and  $\varepsilon$ . We readily obtain

$$\left. \begin{aligned} \frac{\partial}{\partial \varrho} \Pi(\varrho, \varepsilon) &= \frac{1}{\gamma} \int_0^{\varepsilon^2} \frac{dt}{2 t^{3/2}} f(t^{1/2}) \left\{ \Pi\left(\varrho, \varepsilon - \frac{\gamma t}{\varepsilon}\right) - \Pi(\varrho, \varepsilon) \right\} \\ &\quad - \left( \frac{d\varepsilon}{d\varrho} \right)_e \frac{\partial}{\partial \varepsilon} \Pi(\varrho, \varepsilon), \end{aligned} \right\} \quad (3.3)$$

where  $\Pi(\varrho, \varepsilon) d\varrho$  is the probability that a particle with energy parameter  $\varepsilon$  has a range between  $\varrho$  and  $\varrho + d\varrho$ , and where  $\gamma = 4M_1 M_2 / (M_1 + M_2)^2$ . We have seen that in a wide region ( $v < v_1$ , i. e. roughly  $\varepsilon < 10^3$ ), one may write  $(d\varepsilon/d\varrho)_e = k \cdot \varepsilon^{1/2}$ . In equation (3.3) we then have two parameters,  $k$  and  $\gamma$ .

A simple approach to the study of the integral equations (3.1), (3.2) or (3.3) is to obtain from these equations the moments  $\langle R^m \rangle$ , whereby—at least in principle—the probability distribution itself may be determined too.

From (3.1) we obtain directly, when multiplying by  $R^m$  and integrating by parts

$$\left. \begin{aligned} m \langle R^{m-1}(E) \rangle &= \\ N \int d\sigma_{n,e} \left\{ \langle R^m(E) \rangle - \langle R^m(E - T_n - \sum_i T_{ei}) \rangle \right\}. \end{aligned} \right\} \quad (3.4)$$

Similarly, if (3.3) holds we arrive at a somewhat simpler relation

$$\left. \begin{aligned} m <\varrho^{m-1}(\varepsilon)> = & \frac{1}{\gamma} \int_0^{\varepsilon^2} \frac{dt}{2t^{3/2}} f(t^{1/2}) \left\{ <\varrho^m(\varepsilon)> - <\varrho^m\left(\varepsilon - \frac{\gamma t}{\varepsilon}\right)> \right\} \\ & + \left( \frac{d\varepsilon}{d\varrho} \right)_e \cdot \frac{d}{d\varepsilon} <\varrho^m(\varepsilon)>. \end{aligned} \right\} \quad (3.5)$$

By means of equations (3.4) or (3.5) we may successively derive the first, second, etc., moments of the range. In the resulting formulas the equations (3.4) are applied, because they have a wider applicability. In actual evaluations, however, we turn to (3.5), and to the analogous reformulations of (3.6) to (3.13) in  $\varrho - \varepsilon$  variables, although the reformulations are not explicitly stated. Let us ask for the average range  $\bar{R}(E) = < R(E) >$ . According to (3.4)

$$1 = N \int d\sigma_{n,e} \left\{ \bar{R}(E) - \bar{R}(E - T_n - \sum_i T_{ei}) \right\}. \quad (3.6)$$

An obvious procedure in solving (3.6) is to make a series development in powers of  $T = T_n + \sum_i T_{ei}$ . This approximation might seem poor when  $M_1 \sim M_2$ , because  $E - T$  can then take on any value between  $E$  and 0. However, we can profit from the circumstance that the energy transfer to electrons,  $\sum_i T_{ei}$ , is normally quite small, and that the nuclear scattering cross sections (2.9) are strongly forward peaked, since  $f(t^{1/2})t^{-3/2}$  decreases approximately as  $t$  to a power between -1 and -2. We shall presently look into the accuracy of the various approximations.

Take at first only the first order terms in the brackets and denote the corresponding approximation to average range by  $\bar{R}_1(E)$ . We obtain from (3.6)

$$\frac{dR_1(E)}{dE} = \frac{1}{NS(E)}, \quad \bar{R}_1(E) = \int_0^E \frac{dE'}{NS(E')}, \quad (3.7)$$

where  $S(E) = S_n(E) + S_e(E)$  is the total stopping cross section. The formula (3.7) is exactly the straightforward equation (2.2) used in § 2.

Similarly, we can include higher order terms from (3.6),

$$1 = NS(E) \frac{d}{dE} \bar{R}(E) - \frac{1}{2} N \Omega^2(E) \frac{d^2}{dE^2} \bar{R}(E) + \dots, \quad (3.8)$$

where the quantity  $\Omega^2(E) = \int d\sigma_{n,e} T^2$  is related to the straggling. If we include only the second order term we obtain a second order differential

equation which may be solved directly. Still, since the second order term may be considered small, we may express the second derivative by means of  $\bar{R}_1$ . This leads to  $\bar{R}_2(E)$ , the second approximation to average range

$$\bar{R}_2(E) = \int_0^E \frac{dE'}{NS(E')} \left\{ 1 + \frac{\Omega^2(E')}{2} \frac{d}{dE'} \left( \frac{1}{S(E')} \right) \right\}. \quad (3.9)$$

The average square fluctuation in range,  $\overline{\Delta R^2}(E) = \overline{R^2}(E) - \bar{R}^2(E)$ , is obtained from the second moment in (3.4), if we multiply (3.6) by  $2\bar{R}(E)$  and subtract

$$\left. \begin{aligned} \int d\sigma_{n,e} \left\{ \overline{\Delta R^2}(E) - \overline{\Delta R^2}(E - T_n - \sum_i T_{ei}) \right\} = \\ \int d\sigma_{n,e} \left\{ \bar{R}(E) - \bar{R}(E - T_n - \sum_i T_{ei}) \right\}^2. \end{aligned} \right\} \quad (3.10)$$

In this equation the right hand side is a known source term. If we take the same successive steps as in the computation of  $\bar{\varrho}$ , we make a series development in (3.10), in powers of  $T$ . The first terms on both sides of the equation lead to the approximation  $(\overline{\Delta R^2})_1$ ,

$$S(E) \frac{d}{dE} (\overline{\Delta R^2})_1 = \Omega^2(E) \left( \frac{d}{dE} \bar{R}(E) \right)^2, \quad (3.11)$$

where for  $\bar{R}(E)$  we should use the first approximation,  $\bar{R}_1(E)$ . Therefore, also (3.11) brings us back exactly to our previous assumptions in § 2, in this case to (2.4).

Including terms in (3.10) up to second order, we get

$$\left. \begin{aligned} S(E) \frac{d}{dE} (\overline{\Delta R^2}) - \frac{\Omega^2(E)}{2} \frac{d^2}{dE^2} (\overline{\Delta R^2}) = \\ \left( \frac{d}{dE} \bar{R} \right)^2 \Omega^2 - \frac{K(E)}{2} \frac{d}{dE} \left( \frac{d}{dE} \bar{R} \right)^2, \end{aligned} \right\} \quad (3.12)$$

where  $K(E) = \int d\sigma_{n,e} T^3$ . When assuming the new terms in (3.12) to be small, we obtain the second approximation to  $(\overline{\Delta R^2})$ ,

$$\frac{d}{dE} (\overline{\Delta R^2})_2 = \frac{\Omega^2(E)}{S^3(E) N^2} \left\{ 1 + \left( \frac{K}{\Omega^2 S} - \frac{5 \Omega^2}{2 S^2} \right) \frac{dS}{dE} + \frac{1}{2 S} \frac{d\Omega^2}{dE} \right\}. \quad (3.13)$$

By means of the expression (3.13) we are able to estimate the accuracy of the straightforward formulas (3.11) and (2.4). It is important to notice that

TABLE 1  
Comparison of first and second approximation of expansion in  $\gamma$ , for power law scattering. Results for average range and range straggling.

$s$	$\bar{R}_2/\bar{R}_1$	$(\overline{\Delta R^2})_2/(\overline{\Delta R^2})_1$
3/2 .....	$1 + \gamma/24$	$1 + \gamma \cdot 0.10$
2 .....	1	$1 + \gamma/6$
3 .....	$1 - \gamma/15$	$1 + \gamma \cdot 0.14$

the successive approximations made above are simply series expansions of average range and straggling to successive powers of  $\gamma = T_m/E$ .

It is of interest to compare the above approximations. For simplicity let us consider low energies and disregard electronic stopping. Since electronic stopping here tends to diminish fluctuation effects, we obtain in this way slightly exaggerated differences between successive range approximations. Moreover, we use power law scattering cross sections (2.6) or (2.6'). This permits exact computation of  $\bar{R}(E)$ . Note that according to (2.6) the ranges are proportional to  $E^{2/s}$ , while the square straggling in range behaves as  $E^{4/s}$ . We may compare  $\bar{R}_1$ ,  $\bar{R}_2$  and  $\bar{R}$ , and similarly  $(\overline{\Delta R^2})_1$ ,  $(\overline{\Delta R^2})_2$  and  $\overline{\Delta R^2}$ . The results depend on  $\gamma$ , i. e. on the mass ratio. For small values of  $\gamma$ , a series development in powers of  $\gamma$  is accurate. Since  $\gamma$  is often close to its maximum value,  $\gamma = 1$ , we also compare the approximations in this case. The results are listed in Table 1 ( $\gamma < 1$ ) and Table 2 ( $\gamma = 1$ ), in the cases  $s = 3/2$ , 2 and 3. Notice that at low energies values of  $s$  between 2 and 3 are of particular interest.

In the approximation used in Table 1 the range  $\bar{R}_2$  and its fluctuation  $(\overline{\Delta R^2})_2$  are equal to the exact average values  $\bar{R}$  and  $\overline{\Delta R^2}$ , respectively. From Tables 1 and 2 it is apparent that  $\bar{R}_2(E)$  is always a very good approximation to  $\bar{R}(E)$ , and one need not distinguish between the two. The range  $\bar{R}_1(E)$  is somewhat less accurate, but deviates from  $\bar{R}(E)$  by no more than 10 percent in the least favourable case ( $\gamma = 1$ ). In actual range observations the deviation is reduced by electronic stopping and by the change in effective  $s$  with particle energy. There remains a difference between  $\bar{R}_1$  and  $\bar{R}$  only at the lowest values of  $\epsilon$ . For our present purposes where all range curves (e. g. Figs. 3 and 4) are stated in terms of  $\bar{R}_1(E)$  we need hardly distinguish between  $\bar{R}_1(E)$  and  $\bar{R}(E)$ , because of obvious uncertainties in theory and experiment. Still, one might ask why the range curves are computed for  $\bar{R}_1$  in place of  $\bar{R}_2$ . This is simply because a universal range curve would not result when  $\bar{R}_2$  is used.

TABLE 2  
Comparison of first and second approximation with exact formula when  $\gamma = 1$ . Average ranges and range straggling for power law scattering.

$s$	$\bar{R}/\bar{R}_1$	$\bar{R}/\bar{R}_2$	$(\overline{\Delta R^2})/(\overline{\Delta R^2})_1$	$(\overline{\Delta R^2})/(\overline{\Delta R^2})_2$
3/2 .....	1.053	1.01	1.03	0.94
2 .....	1	1	1.20	1.03
3 .....	0.904	0.97	1.26	1.10

The straggling approximations  $(\overline{\Delta R^2})_1$  and  $(\overline{\Delta R^2})_2$  are, as a rule, a little smaller than  $\overline{\Delta R^2}$  when  $\gamma = 1$ . This deviation becomes quite pronounced if instead we consider the relative straggling in range. Thus, in the extreme cases of  $s = 3$  and  $\gamma = 1$  we have  $(\overline{\Delta R^2})_1/\bar{R}_1^2 = 0.133$  according to (2.13), while  $\overline{\Delta R^2}/\bar{R}^2 \approx 0.20$  for  $\gamma = 1$  and  $2 < s < 3$ . At quite low values of  $\epsilon$ , and  $\gamma = 1$ , the straggling in Fig. 6 is therefore somewhat lower than the straggling in average range; still it is noteworthy that the electronic stopping has a considerable influence on straggling also for quite low values of  $\epsilon$ . We infer moreover that the absolute values of range straggling in Fig. 7 are expected to represent  $\overline{\Delta R^2}$  quite accurately, i. e. they are superior to the relative straggling values in Fig. 6. Note that the deviations are only important when  $\gamma \approx 1$ . The outcome of the discussion in the present chapter is therefore that the simple quantities  $\bar{R}_1$  and  $(\overline{\Delta R^2})_1$ , introduced already in § 2, are satisfactory estimates of average range and average square fluctuation in range.

#### Results for power law scattering

In the interesting case of power law scattering, (2.6'), the formula (3.3) takes a particularly simple form if electronic stopping is neglected. In fact, we then obtain

$$\frac{\partial}{\partial r} P(r, \epsilon) = \int_0^1 \frac{dy}{y^{1+1/s}} \left\{ (1 - \gamma y)^{-2/s} P(r \cdot [1 - \gamma y]^{-2/s}, \epsilon \cdot [1 - \gamma y]) - P(r, \epsilon) \right\}, \quad (3.13)$$

where  $r = \lambda_s \varrho \cdot (2\gamma\epsilon^{2/s})^{-1}$  and  $\int_0^\infty P(r, \epsilon) dr = 1$ . If the power law holds down to zero energy, equation (3.13) permits us to choose  $P(r, \epsilon)$  independent of  $\epsilon$ , and an extremely simple recursion formula is obtained for the moments of the distribution,

$$m < r^{m-1} > = < r^m > \cdot I(\gamma, m, s), \quad I(\gamma, m, s) = \int_0^1 \left( 1 - (1 - \gamma y)^{2m/s} \right) \frac{dy}{y^{1+1/s}}. \quad (3.14)$$

The moments therefore only depend on one parameter,  $\gamma$ , for any given power law scattering.

This result, where virtually the whole range distribution is determined immediately for any energy when merely the power  $s$  is stated (and  $\gamma$  is known), is

clearly a direct consequence of universal cross sections,  $f(l^{1/2})$ . In a more qualitative sense, it is apparent that if at one particle energy a cross section is given as a function of  $T/T_m = \sin^2 \theta/2$ , this cross section leads to a certain ion-atom potential from which the scattering at all lower energies may be derived. This circumstance is expressed in an approximate way by the unified cross section, (2.9), and the results happen to be analytically simple for a power law cross section.

The integral  $I(\gamma, m, s)$  may be expressed by means of the incomplete beta function (cf. ERDÉLYI et al. (1953)),

$$I(\gamma, m, s) = -s \left\{ 1 - (1 - \gamma)^{2m/s} \right\} + 2m\gamma^{1/s} B_\gamma \left( 1 - \frac{1}{s}, \frac{2m}{s} \right), \quad (3.15)$$

and is particularly simple when  $\gamma \ll 1$ , in which case a power series in  $\gamma$  converges rapidly,

$$\left. \begin{aligned} I(\gamma, m, s) &= \frac{2m\gamma}{s-1} \left\{ 1 - \frac{\gamma}{2s} \frac{s-1}{2s-1} (2m-s) \right. \\ &\quad \left. + \frac{\gamma^2}{3s^2} \frac{s-1}{3s-1} (2m-s)(m-s) + \dots \right\}, \quad \gamma \ll 1. \end{aligned} \right\} \quad (3.16)$$

An interesting case is also  $\gamma = 1$ , where the incomplete beta function in (3.15) becomes the usual beta function  $B_1(p, q) = \Gamma(p)\Gamma(q)/\Gamma(p+q)$ .

The results in (3.14), (3.15) and (3.16) were used in Tables 1 and 2 for the computation of the first and second moments in various approximations. It is easy to derive also higher moments.

#### § 4. Projected Ranges and Associated Quantities

##### Average projected range

An interesting quantity appears to be the projection of the range on the initial direction of the particle path. This quantity is often observed directly. Thus, one might be concerned with a collimated beam of particles passing through a number of foils perpendicular to the direction of the beam; the number of particles collected in each foil gives just the distribution in range projected on the initial direction of the beam. We may, in fact, define the concept of projected range as follows. A particle starts inside an infinite homogeneous medium from the origin in the direction of the  $x$ -axis; the value of  $x$  for the end point of the path is the projected range,  $R_p$ . The distribution in  $x$  is the distribution in projected range. Quantities of particular interest here are the average projected range,  $\bar{R}_p = \bar{R}_p(E)$ , and the average straggling in projected range,  $\overline{\Delta R_p^2} = \bar{R}_p^2 - \bar{R}_p^2$ .

An integral equation for the average projected range may be obtained in analogy to the derivation of (3.1). We find readily

$$1 = N \int d\sigma_{n,e} \{ \bar{R}_p(E) - \bar{R}_p(E-T) \cos \varphi \}, \quad (4.1)$$

where  $T = T_n + \sum_i T_{ei}$ , and  $\varphi$  is the deflection of the ion in the laboratory system. There is a close similarity to the integral equation (3.6) for the average range, the only difference being the factor  $\cos \varphi$  in (4.1).

Let us consider some approximations which can be useful in solving (4.1). If always  $T \ll E$ , i. e.  $\gamma \ll 1$ , or if  $\bar{R}_p$  is nearly proportional to  $E$ , we may write

$$1 = \bar{R}_{p1}(E) N \int d\sigma_{n,e} (1 - \cos \varphi) + \frac{d\bar{R}_{p1}(E)}{dE} N \int d\sigma_{n,e} \cdot T \cdot \cos \varphi. \quad (4.2)$$

This approximation is similar to the one for  $\bar{R}_1$  in (3.7) and (2.2), and we therefore use the notation  $\bar{R}_{p1}$  for the projected range in (4.2). Actually, if the deflection  $\varphi$  may be neglected, we obtain  $(d\bar{R}_{p1}/dE) = N \cdot S$ , i. e.  $\bar{R}_{p1}$  becomes equal to  $\bar{R}_1$ .

When solving (4.2) we can introduce the familiar transport mean free path,  $\lambda_{tr}$ , and a transport stopping cross section,  $S_{tr}$ ,

$$\frac{1}{\lambda_{tr}} = N \int d\sigma_{n,e} (1 - \cos \varphi), \quad S_{tr} = \int d\sigma_{n,e} T \cos \varphi. \quad (4.3)$$

With this notation, equ. (4.2) becomes

$$1 = \frac{\bar{R}_{p1}(E)}{\lambda_{tr}(E)} + \frac{d\bar{R}_{p1}(E)}{dE} \cdot NS_{tr}(E), \quad (4.4)$$

which equation (4.4) has the solution

$$\bar{R}_{p1}(E) = \int_0^E \frac{dE'}{NS_{tr}(E')} \exp \left\{ \int_E^{E'} \frac{dE''}{\lambda_{tr}(E'') N \cdot S_{tr}(E'')} \right\}, \quad (4.5)$$

and this result should be a good approximation to  $\bar{R}_p(E)$  if  $\gamma$  is small, or if  $R_p$  is nearly proportional to energy. We may solve the equation for  $\bar{R}_p$  in the lowest approximation. This corresponds to taking the leading term in a series development in  $\mu = M_2/M_1$ , assuming  $\mu$  to be small. The approximation is similar to that in § 3, for  $\gamma \ll 1$ . In the limit of small  $\mu$ , the angle  $\varphi$  is always small and we need only include  $\varphi^2$ -terms in (4.3). Using

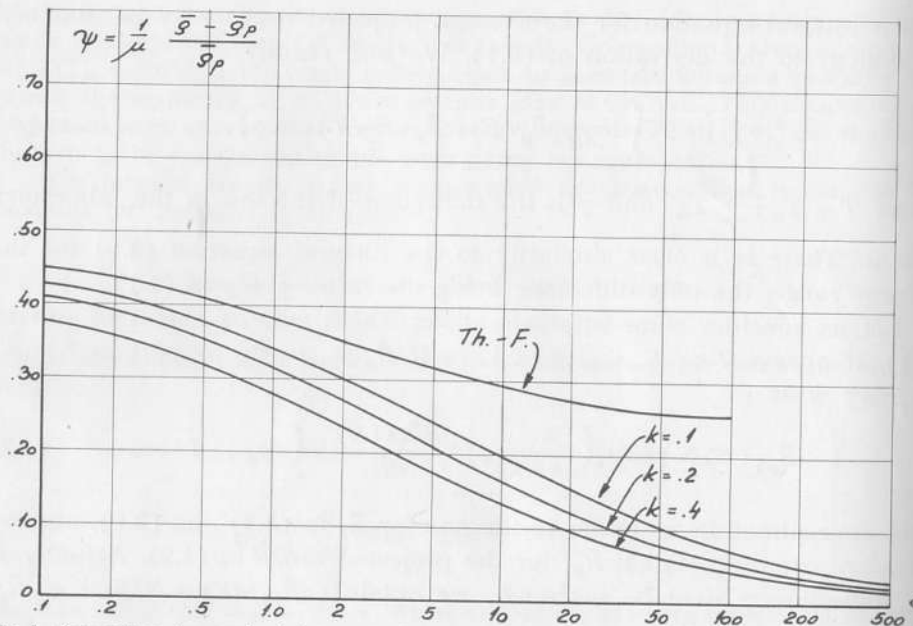


Fig. 8. Correction for projected ranges  $(\bar{R}_1 - \bar{R}_{p1})/\bar{R}_{p1} = \mu\psi$ , to first order in the mass ratio  $\mu = M_2/M_1$ . Curves are shown for pure nuclear stopping and for three values of electronic stopping parameter  $k$ .

the nuclear scattering cross section (2.9) and electronic stopping  $(d\epsilon/d\varrho)_e = k \cdot \epsilon^{1/2}$ , we have computed the first order correction from average projected range to average range along the path. The resulting curves are shown in Fig. 8, for various values of  $k$ , and also for pure nuclear stopping.

It is more difficult to obtain accurate approximations to  $\bar{R}_p$  when  $\mu$  is large, corresponding to large angles of scattering,  $\varphi$ . We use the approximate equation (4.5) and profit from the circumstance that  $\bar{R}_p$  is not far from being proportional to energy. By means of (2.9), solutions were obtained for  $\mu = 1$  and  $\mu = 2$ , and a few representative values of the electronic stopping parameter  $k$ . The results are shown in Fig. 9.

The power law approximation of nuclear scattering, (2.6), with neglect of electronic stopping, permits accurate solutions for  $\bar{R}_p$ . We utilize the circumstance that  $\bar{R}_p \propto E^{2/s}$ . As an example, we consider the useful case of  $s = 2$ . The exact solution of (4.1) and (3.6) leads to (LINDHARD and SCHARFF (1961))

$$\bar{R}/\bar{R}_p = \frac{1}{4} \left\{ -1 - 3\mu + (5 + \mu) \frac{1 + \mu}{2\mu^{1/2}} \arccos \frac{1 - \mu}{1 + \mu} \right\} \approx 1 + \frac{1}{3}\mu, \quad s = 2. \quad (4.6)$$

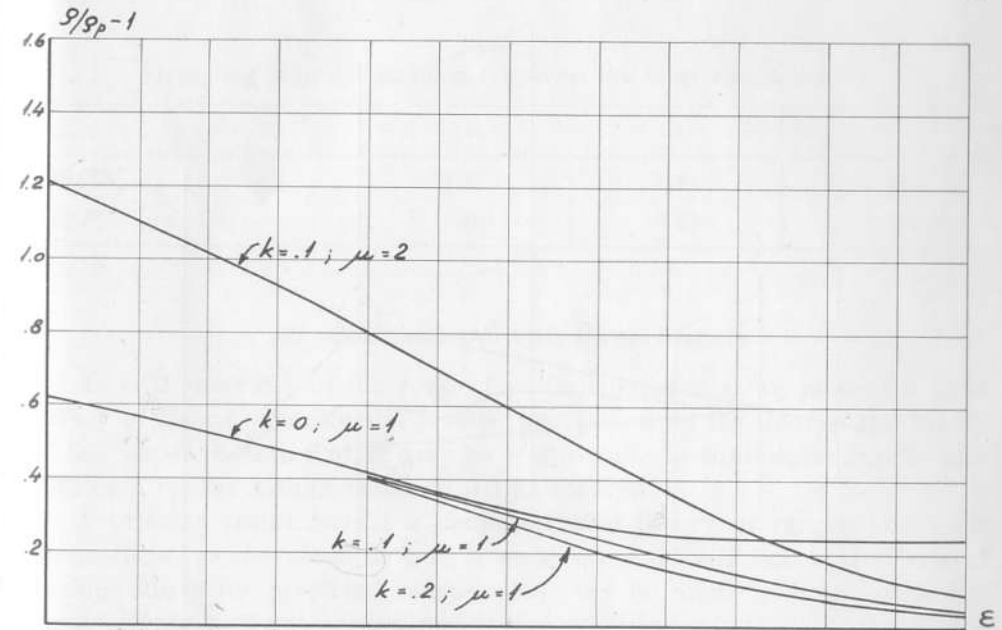


Fig. 9. Approximate curves for  $\bar{R}_1/\bar{R}_{p1}$  for large values of the ratio  $\mu = M_2/M_1$  and a few values of  $k$ .

As may be seen from Fig. 8, the rule-of-thumb  $\bar{R}/\bar{R}_p = 1 + \mu/3$  is a fair approximation at low energies.

As a further example we may quote the value of  $\bar{R}/\bar{R}_p$  for small  $\mu$ , and any value of  $s$ ,

$$\bar{R}/\bar{R}_p \approx 1 + \mu \frac{s^2}{4(2s-1)}, \quad (4.7)$$

which approximation is quite accurate up to  $\mu \sim 1$ .

#### Associated range concepts

The average projected range is determined by one closed equation. However, the equations governing the higher moments of the projected range are far more complicated. If we treat the average square of the projected range,  $\bar{R}_p^2$ , we must also introduce the average square of the range projected on the plane perpendicular to the initial direction,  $\bar{R}_1^2$ . The average square of the distance between the starting-point and the end point of the path is then  $\bar{R}_c^2 = \bar{R}_p^2 + \bar{R}_1^2$ . We may describe  $R_c$  as the chord range (also referred to as vector range). These range concepts are illustrated in Fig. 10.

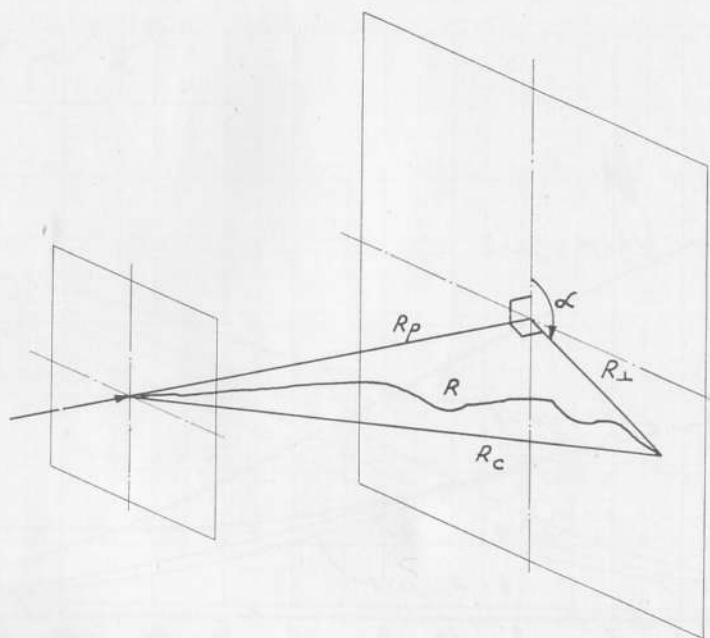


Fig. 10. Sketch illustrating definition of range concepts  $R$ ,  $R_p$ ,  $R_c$  and  $R_{\perp}$ .

The integral equations for  $\overline{R_p^2}$  are derived in a similar way as (3.1). The following two equations are obtained, after rearrangement of terms,

$$2 \bar{R}_p(E) = N \int d\sigma_{n,e} \{ \overline{R_c^2}(E) - \overline{R_c^2}(E-T) \}, \quad (4.8)$$

$$2 \bar{R}_p(E) = N \int d\sigma_{n,e} \left\{ \overline{R_r^2}(E) - \left(1 - \frac{3}{2} \sin^2 \varphi\right) \overline{R_r^2}(E-T) \right\}, \quad (4.9)$$

where

$$\overline{R_c^2} = \overline{R_p^2} + \overline{R_{\perp}^2} \text{ and } \overline{R_r^2} = \overline{R_p^2} - \frac{1}{2} \overline{R_{\perp}^2}. \quad (4.10)$$

The two equations (4.8) and (4.9) may be solved separately, and then  $\overline{R_p^2}$  is found from (4.10).

First order solutions of (4.8) and (4.9), for  $\mu \ll 1$ , can be obtained in a direct manner. However, we shall merely consider the case of power law scattering, with neglect of electronic stopping. The exact solutions may then be expressed as beta functions. In Table 3 we quote the results for  $\mu = 1$  and various values of  $s$ . It is seen that in these cases  $\Delta \overline{R_p^2}$  is of order of  $\Delta \overline{R^2}$ .

TABLE 3  
Straggling in projected range for power law scattering and  $\mu = 1$ .

$s$	3/2	2	3
$\Delta \overline{R^2}/\Delta \overline{R_p^2}$ .....	1.25	1.33	1.38
$\Delta \overline{R_p^2}/\overline{R_p^2}$ .....	0.204	0.275	0.341

### § 5. Comparison with Experiments

As an illustration of the connection to experiments, we present a brief survey of recent experimental results, interpreted on the lines of the theory of this paper. Before that, it may be worth-while to summarize briefly and comment on the salient features of this theory.

A primary result is that a simple-minded theory of ranges and their fluctuations, as described in § 2, is quite accurate and that corrections of various kinds for projected ranges, etc., may be made without much difficulty, if necessary. A second result, somewhat independently of the details of the theory of collisions, is that a  $\varrho - \varepsilon$  plot is useful for a study of ranges of particles with  $\varepsilon < 1000$ , and particularly for  $\varepsilon \lesssim 10$ . A third result is that for any ion of high energy a range correction,  $\Delta$ , for the effect of nuclear stopping has been obtained, which permits a more accurate study of electronic stopping. Fourth, e. g. various isotope effects can serve to check several details of the theory, as may also observations of range straggling.

A theoretical result of special interest is that for  $Z_1 = Z_2$  the electronic stopping constant is  $k \sim 0.15$ , except when  $Z_1 = 1$ . Therefore, the range energy curve for  $Z_1 = Z_2$  should be closely a single curve in a  $\varrho - \varepsilon$  plot. However, the corrections for e. g. projected ranges are not negligible in this case.

The numerical results computed here are based on a much simplified model of collisions. It is certainly possible to introduce a more detailed description of the collisions (cf. Notes on Atomic Collisions I and IV), and thereby improve on the present theoretical results. However, it may be more important to remove uncertainties and to correct misconceptions in the theory by measurements of range and stopping.

Another important circumstance is that direct comparisons with measured ranges may be made preferably in gases, where successive collisions are uncorrelated. In several respects stopping in solids may also answer the purpose, but experiments at low ion energies clearly seem to indicate the

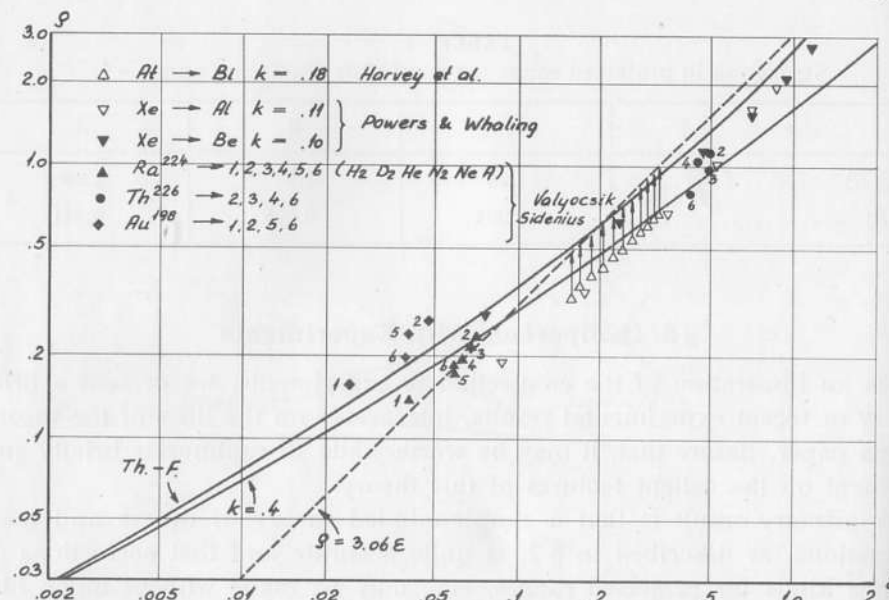


Fig. 11. Comparison between theoretical curves for  $\bar{\eta}_1(\epsilon)$  given by (2.2), (2.9), (2.10) and (2.11), and measurements for  $\epsilon < 2$ . As indicated on the figure, numbers 1, 2, 3, 4, 5 and 6 refer to stopping gases H<sub>2</sub>, D<sub>2</sub>, He, N<sub>2</sub>, Ne and A, respectively. For further comments cf. text.

kind of correlation of collisions described as tunnelling (cf. PIERCY et al. (1963)), with strong directional effects and range lengthening in certain crystal structures. Although these range effects are in themselves highly interesting, their special character make them less suited in a general first comparison between range theory and experiments. In e. g. amorphous solids the effect appears to be absent, as was to be expected.

It should be appreciated that in the following we have merely made a compilation of measurements; not all of them are plotted in the figures. We are not in a position to make any critical examination of the experiments, some of which are in mutual disagreement or obviously inaccurate. We have included primarily the more recent measurements. A review of previous observations is given by HARVEY (1960). We are mainly interested in experiments where nuclear stopping is dominating, and do not discuss electronic stopping. NORTHCLIFFE (1963) has given a valuable survey of measurements on stopping in the energy region just above the one considered here, i. e. when electronic stopping dominates and goes through a maximum.

In plotting the results we have made approximate corrections for projected ranges, etc. Normally, the range measurements are plotted directly

on the figures, and range corrections are indicated by arrows. In some cases our knowledge of the measurements was too scanty to permit a range correction. As a general rule, we have corrected for projected ranges, etc., only if the correction exceeds  $\sim 10$  percent.

Fig. 11 shows the theoretical range curve for values of  $\epsilon$  smaller than 2, where nuclear stopping is quite dominating. The ranges for pure nuclear stopping are given by the upper solid curve, denoted as Th.-F. on the figure. A curve for exceptionally large electronic stopping, i. e.  $k = 0.4$ , is also shown. The actual  $k$ -values are quite small, and thus the expected ranges should be close to the Th.-F. curve. Further, note the dashed straight line corresponding to range proportional to energy,  $\eta = 3.06\epsilon$ . It should be emphasized that for extremely low energies,  $\epsilon \lesssim 10^{-2}$ , the theoretical curve is not too well-defined.

HARVEY, WADE and DONOVAN (1960) observed projected ranges for At<sup>205</sup> and At<sup>207</sup> ions in bismuth. The At recoil ions were produced by  $\alpha$ -bombardment of a bismuth foil, leading to an  $(\alpha, xn)$  process. This resulted in At ions with various energies between 400 and 900 keV; the energies were not sharply defined. Approximate corrections for projected range are shown by arrows in Fig. 11. The observations of HARVEY, WADE and DONOVAN are in satisfactory accord with the predicted ranges.

POWERS and WHALING (1962) studied projected ranges of monoenergetic ions of nitrogen and inert gases in several solids. The depth of penetration of the ions was obtained from a subsequent analysis of the distribution in angle and energy loss of protons scattered from the ions imbedded in the target. The ranges of POWERS and WHALING are generally in good agreement with the theoretical curves. In the figure, we have included only their range measurements for Xe in Be and in Al. The corrections for projected ranges are quite small and are omitted. The ranges in Al may be compared with those of DAVIES et al. in Fig. 12. These two range observations for Xe in Al give quite different results and are placed on either side of the theoretical curve.

VALYOCSEK (1959) made accurate observations of ranges of Ra<sup>224</sup> and Th<sup>226</sup> recoil atoms with, respectively, 97 and 725 keV energies. Ranges are measured in gases using the electrostatic collection technique of GHIORSO and SIKKELAND. Ranges and range straggling were observed in deuterium, helium, nitrogen and argon, and in hydrogen and neon (only for Ra ions). The observations are shown in Fig. 11. They are in good agreement with theory (between 0 and 20 percent below theoretical ranges), and correspond to  $k = 0.12$ , except in hydrogen where  $k = 0.16$ .

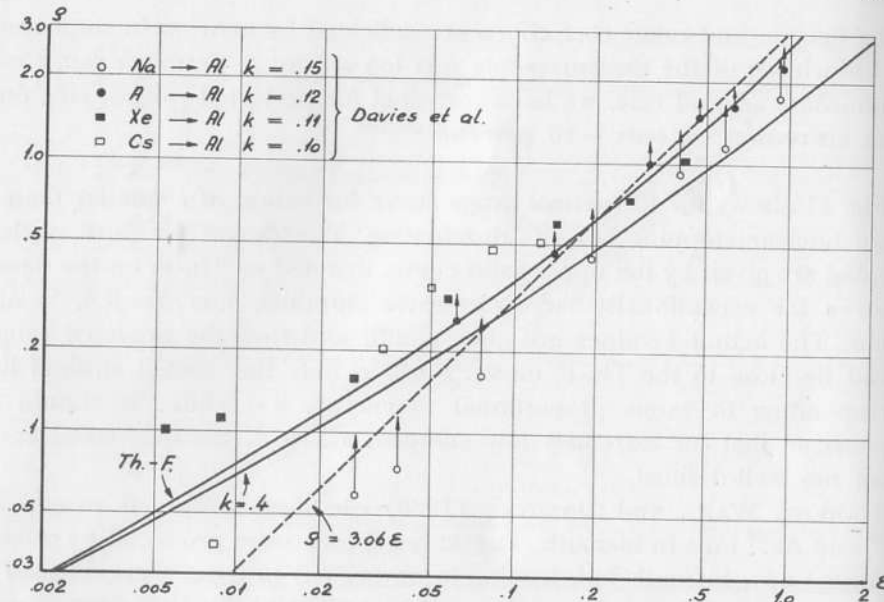


Fig. 12. As Fig. 11; measurements of median ranges by DAVIES et al. in Al. Ranges at low energies exceed theoretical curves, probably as an effect of tunnelling in crystal lattice.

A few measurements by the Copenhagen group (SIDENIUS, private communication) are also included in Fig. 11. The projected range of  $\text{Au}^{198}$  ions of energy 50 keV is measured by electrostatic collection. The correction for projected range is negligible. The ranges are slightly above theoretical curves. The  $k$ -values are as in VALYOCSIK's measurements.

DAVIES et al. (1960, 1961 and private communication) have observed projected ranges in Al, for the following ions:  $\text{Na}^{24}$ ,  $\text{A}^{41}$ ,  $\text{K}^{42}$ ,  $\text{Rb}^{86}$ ,  $\text{Xe}^{133}$  and  $\text{Cs}^{137}$ . Monoenergetic radioactive ions of energies between 1 keV and 2 MeV enter a polished Al surface. Thin layers of Al are removed successively by electro-chemical means and the residual activity is measured. In this way the distribution in projected range is obtained. The range values of DAVIES et al. in Fig. 12 are median ranges. At the higher energies there is good agreement with theoretical curves.

The measurements by DAVIES et al. were made with polycrystalline Al. It has turned out that the structure of Al is such that tunnelling of the ions may occur, whereby the average range becomes considerably larger than for a random system, and the range distribution has an exponential tail (PIERCY et al. (1963)). The results of PIERCY et al. for  $\text{Kr}^{85}$  in Al and  $\text{Al}_2\text{O}_3$  at 40 keV are compared with theoretical estimates in Table 4. There is

TABLE 4

Ranges (in  $\mu\text{g}/\text{cm}^2$ ) of 40 keV  $\text{Kr}^{85}$  in Al and  $\text{Al}_2\text{O}_3$ , and average square straggling in range. Experimental results by PIERCY et al. Computed results (columns 3 and 5) are for random system, as indicated.

	$R_{exp}^{med}$	$\bar{R}_{exp}$	$\bar{R}_{rand}$	$(\Delta R)^2_{exp}$	$(\Delta R)^2_{rand}$
Al.....	9.0	11.5	7.1	91	4.6
$\text{Al}_2\text{O}_3$ .....	7.7	7.7	6.5	7.8	3.5

satisfactory agreement in the amorphous substance  $\text{Al}_2\text{O}_3$ , both as regards ranges and straggling. It appears also from Table 4 that the experimental median range in Fig. 12 is probably somewhat larger than the average ranges of a random system of Al atoms. We therefore infer that the results of DAVIES et al. in Fig. 12 are not in contradiction to the theoretical ranges of a random system. Note the very large experimental range straggling in Table 4 for Al, characteristic of an exponential distribution, where  $\overline{\Delta R^2} = \bar{R}^2$ .

There are several other measurements in the regions of energy corresponding to Figs. 11 and 12. Thus, BAULCH and DUNCAN (1957) obtain ranges of  $\alpha$ -recoils ( $\varepsilon \lesssim 0.1$ ) from 0 to 10 percent below theoretical curves. The results of VAN LINT et al. (1961) are at the higher energies at least about a factor of 2 above theoretical expectations, while at lower energies ( $\varepsilon \sim 0.04$ ) agreement is fair. However, these measurements show a very considerable scatter. GUSEVA, INOPIN and TSYTKO (1959) measured ranges of monoenergetic  $\text{Si}^{30}$  ions in Ta and Cu backings, at energies between 10 and 25 keV. The depth of penetration was estimated from proton energies necessary for a  $(p, \gamma)$  process, together with knowledge of proton stopping. Their results are about a factor of 2 above the theoretical curves.

Fig. 13 shows some observations for  $1 < \varepsilon < 100$ , and corresponds to Fig. 4 in § 2. We are here in a region where the electronic stopping begins to take over. It is then important to know the value of the constant  $k$ . Some of the projected ranges observed by POWERS and WHALING (1962) are shown in Fig. 13, including one where the ratio  $\mu = (M_2/M_1) \sim 2$ , i. e. the corrections for projected range are large. The agreement with theoretical curves is good.

WINSBERG and ALEXANDER (1961) and ALEXANDER and SISSON (1962) measured projected ranges for  $\text{Tb}^{149}$  ions in aluminium, at energies between 4 and 30 MeV, and for At and Po ions in aluminium and gold, at energies between 3.5 and 13 MeV. The projected ranges and the range stragglings were obtained from the activities in stacks of catcher foils. In Fig. 13 we have included results for At and Po in gold and for  $\text{Tb}^{149}$  in

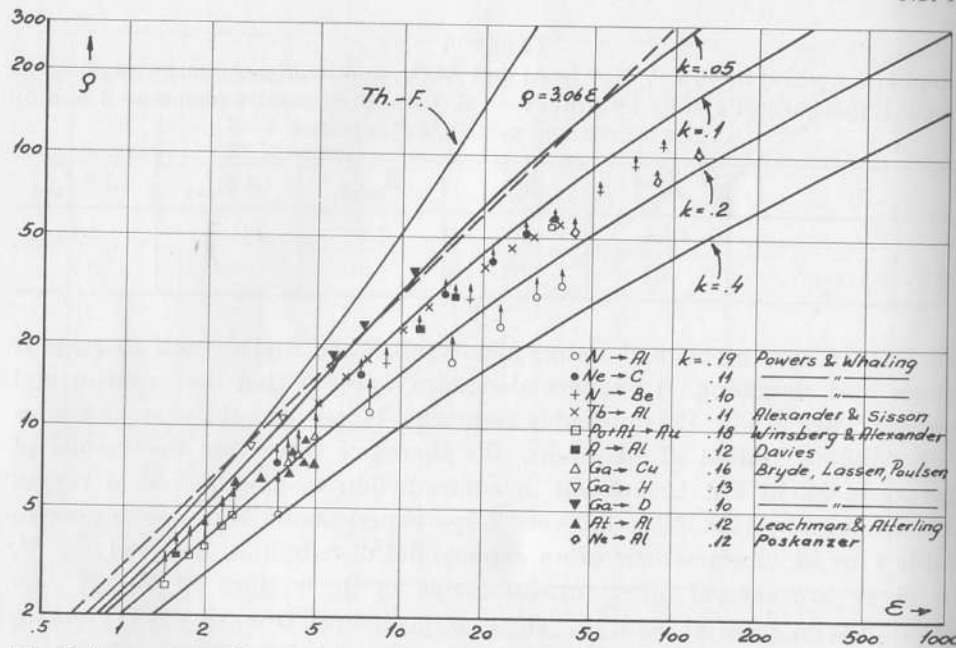


Fig. 13. Comparison with range measurements in the region  $1 < \epsilon < 100$ , where electronic stopping becomes important. Theoretical  $k$ -values are given, indicating the theoretical curve with which to compare the observations.

aluminium. There is good agreement with the theoretical curves. It may be noted that the ions were formed in a nuclear reaction with subsequent neutron evaporation.

In the case of  $A^{41}$  in aluminium, DAVIES et al. (private communication) performed measurements at energies so high that electronic stopping is important. The ranges are in good agreement with the theoretical curves in Fig. 13.

BRYDE, LASSEN and POULSEN (1962) measured projected ranges for radioactive  $Ga^{66}$  recoil ions in gases using electrostatic collection. As typical representatives of their observations we have in Fig. 13 included ranges in hydrogen and deuterium. These ranges are about 40 percent above theoretical ranges. BRYDE, LASSEN and POULSEN also observed projected ranges for  $Ga^{66}$  in copper; the latter ranges are in good agreement with the theoretical curve. Also included in Fig. 13 are three measurements by POSKANZER (1963) of 1–3 MeV  $Ne^{22}$  ions in aluminium; these ranges are smaller than theoretical ranges. Finally, in Fig. 13 is shown the early measurements of ranges by LEACHMAN and ATTERLING (1957), where recoil ions of  $At^{203}$

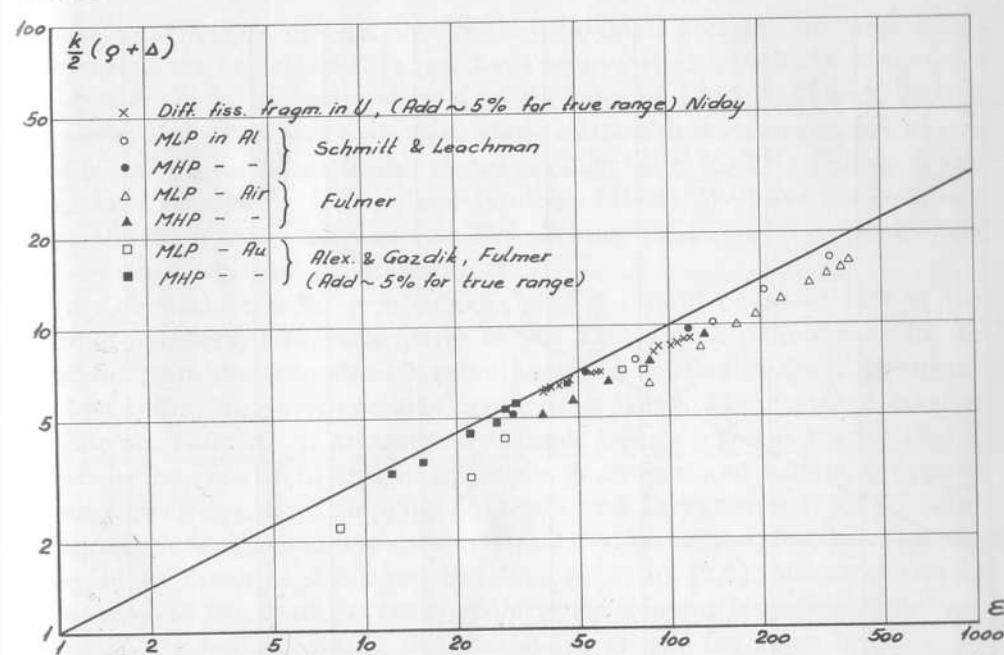


Fig. 14. Comparison between theoretical curve and range measurements for fission fragments, nuclear stopping being eliminated. For large values of  $\epsilon$  the representation shown here is superior to that in Fig. 13.

and  $At^{205}$  penetrated a stack of aluminium foils, and projected ranges were measured. There is fair agreement, but apparently some fluctuations between individual measurements.

As mentioned previously, in the present paper we do not attempt a systematic study of electronic stopping as obtained from measurements at high values of  $\epsilon$ . We may merely show two sets of representative measurements, where the nuclear stopping is eliminated, so that the extrapolated electronic range is obtained. For  $v < v_1$  the theoretical extrapolated electronic range is  $\varrho_e = 2\epsilon^{1/2}/k$ . Using theoretical range corrections for nuclear stopping,  $\Delta(k, \epsilon)$ , as indicated in Fig. 5, we have plotted in Figs. 14 and 15 values of  $(k/2)\{\varrho + \Delta(k, \epsilon)\}$  obtained from measurements of  $\varrho$ . The theoretical curve is the straight line  $k\varrho_e/2 = \epsilon^{1/2}$ . Fig. 14 contains only measurements of ranges of fission fragments. In Fig. 14 is shown measurements by NIDAY (1961) of fission fragment ranges in uranium. NIDAY used a thick uranium foil packed in aluminium catcher foils. Fission fragments resulted from thermal neutrons. The fragments ending up in aluminium were separated by radiochemical means. In this way an estimate of the ranges along the

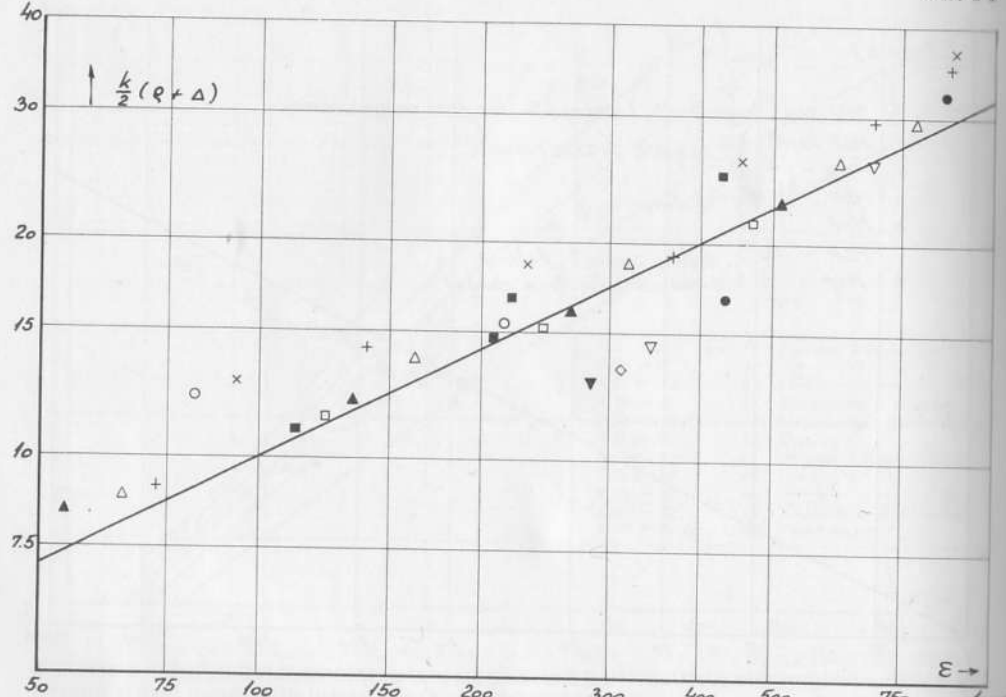


Fig. 15. Some recent measurements of projected ranges for light atoms in gases, corrected for nuclear stopping only, like in Fig. 14. Full-drawn curve is theoretical range  $\epsilon^{1/2}$ . Points stand for following ions in air:  $\times$  Li,  $+$  B,  $\triangle$  C,  $\Delta$  O,  $\square$  F,  $\blacksquare$  Ne,  $\circ$  Na, and following ions in argon:  $\bullet$  Li,  $\nabla$  B,  $\blacktriangledown$  N (measurements by TEPLOVA et al.). Further,  $\diamond$  indicates F in nitrogen, measured by BRYDE, LASSEN and POULSEN.

chord was obtained. The ranges of NIDAY should be corrected by approximately +5 percent in order to obtain true ranges. The agreement with the theoretical range is good.

In Fig. 14 is also included observations on fission fragment ranges by ALEXANDER and GAZDIK (1960), FULMER (1957) and LEACHMAN and SCHMITT (1954). In the case of gold, about 5 percent should be added in order to obtain true ranges. There is agreement within  $\sim 10$  percent.

A number of other authors have measured ranges of fission fragments (SMITH and FRANK (1959), KATCOFF, MISKEI and STANLEY (1948), GOOD and WOLLAN (1956), BØGGILD, ARRØE and SIGURGEIRSSON (1947), DOUTHET and TEMPLETON (1954), SUZOR (1949), PORILE and SUGARMAN (1957), cf. also the review article by HARVEY (1960)). Some of the earlier measurements may be less accurate than those shown in Fig. 14, but generally there is approximate agreement with theory.

As an example of light ions with substantial energies we have taken measurements of projected ranges by TEPLOVA et al. (1962). A number of ions, from Li to Na, with energies in the interval 1–10 MeV, were slowed down in air, argon and hydrogen. Many of these measurements are shown in Fig. 15. On the figure is also shown a range value for  $F^{18}$  in nitrogen gas, measured by BRYDE, LASSEN and POULSEN (1962). We have not indicated corrections for projected ranges on Fig. 15, since the largest correction would be  $\sim +8$  percent (for Li in argon gas).

In connection with electronic stopping it should be noted that at low atomic numbers, and particularly at low values of  $Z_1$ , there may be deviations from the theoretical  $k$ -value based on a Thomas-Fermi treatment. At low atomic numbers one may expect variations in the measured  $k$ -values due to shell effects. As an extreme example from a Thomas-Fermi point of view, in the case of Li ions in hydrogen, deuterium and helium, it appears from measurements of stopping (ALLISON and LITTLEJOHN (1957)) and of ranges (CLERC, WÄFFLER and BERTHOLD (1961)) that the electronic stopping may be as much as 2–3 times less than given by (2.5). Measurements by ORMROD and DUCKWORTH (1963) of electronic stopping in carbon for all ions with  $Z_1 \lesssim 11$  indicate minor shell variations around the value in (2.5).

#### Range straggling

As to straggling in range (cf. p. 14) we have not attempted any closer analysis. High accuracy is difficult to obtain in range straggling, and at low  $\epsilon$ -values ( $\epsilon < 0.5$ ) the rule-of-thumb  $(\Delta \rho/\rho)^2 = \gamma/6 = M_1 M_2 (M_1 + M_2)^{-2} \cdot (2/3)$  is often sufficient. In many experiments a considerable fluctuation was present in the initial ion beam, e. g. because the ion resulted from a compound nucleus after neutron evaporation. The experimental range stragglings are often considerably above the curves. The measurements by VALYOCSIK on 97 keV  $\alpha$ -recoils (cf. HARVEY (1960)) correspond to rather well-defined conditions. For 97 keV Ra the straggling in nitrogen, neon and argon is comparable with the theoretical one (cf. Fig. 6), but in the light gases, hydrogen, deuterium and helium, the straggling is much in excess of theoretical estimates. When subtracting a common constant of order of 0.016 from the experimental straggling  $(\Delta \rho)^2_{exp}$ , one obtains a relative straggling  $\gamma^{-1} (\Delta \rho/\rho)^2 \approx 0.14-0.18$ , in excellent agreement with theory (since  $\epsilon \approx 0.03-0.07$ , and  $k \approx 0.12$ ). For 725 keV Th ions, where  $\epsilon \approx 0.4-0.5$ , the experimental relative straggling is much too large in deuterium and helium. A reduction of  $(\Delta \rho)^2_{exp}$  by  $\approx 0.04$  in all gases would give a reasonable order of magnitude of the straggling. As a further example, many measurements by the Copen-

hagen group show rather large straggling effects, but some results (e. g. ranges of 50 keV Ga<sup>66</sup> in hydrogen, helium, nitrogen and argon, shown in Fig. 11) with  $\epsilon \approx 0.3-0.5$ , have a straggling  $(\Delta\varrho/\varrho)^2 \gamma^{-1} \approx 0.15-0.25$ . Even in the difficult case of the lightest gases, where the theoretical straggling is extremely small, there is reasonable accord with theory.

### Isotope effects

It is of interest to study isotope effects in range measurements. We shall treat the question of different isotopes used as stopping medium\*. Although electronic stopping may dominate in the value of the range itself, isotope effects can still give direct information about the nuclear stopping. An instructive example is provided by the measurements of BRYDE, LASSEN and POULSEN (1962, and private communication). They observed ranges of Ga<sup>66</sup> in hydrogen and deuterium; at high energies  $R_D$  is slightly larger than  $R_H$ , while at low energies  $R_H$  exceeds  $R_D$ . Now, if there was only electronic stopping, the two ranges would be equal, so that differences are due to nuclear stopping. It is seen from (2.7) that the nuclear stopping behaves as  $S_n \propto M_2^{1-2/s}$ , when  $M_1 \gg M_2$ . At quite low energies, where the ion cannot penetrate deeply into the atom, the effective power of the potential is of order of  $s = 3$ , and thus  $S_{nD} > S_{nH}$ . At high energies, where the screening is weak, the effective power approaches  $s = 1$ , and therefore  $S_{nH} > S_{nD}$  (LINDHARD and SCHARFF (1961)). According to Fig. 2, the change-over in stopping occurs at an  $\epsilon$ -value smaller than 0.5. Correspondingly, in Fig. 4 the change-over in slope—from lower to higher than that of the straight dashed line—occurs at  $\epsilon \sim 1$  for the Th.-F. curve.

Instead of this qualitative explanation of experimental results we may directly compare experimental range differences with theoretical ones deduced from Figs. 3 and 4. The results are shown in Table 5. Agreement between theoretical and experimental range differences is quite good,

TABLE 5

Differences between ranges in D<sub>2</sub> and H<sub>2</sub> for Ga<sup>66</sup> ions. Ranges are in mm at 300° K, 760 mm Hg.

Energy (keV)	1190	790	610	50
$(R_D - R_H)_{th}$ .....	0.9	0.7	0.6	-0.05
$(R_D - R_H)_{exp}$ .....	1.5	0.8	0.5	-0.05

\* A measurement, where different isotopes are chosen for the incoming particle, is discussed by LINDHARD and SCHARFF (1961).

especially at the lower energies. This result is obtained in spite of the fact that at the three higher energies the absolute ranges of BRYDE, LASSEN and POULSEN are as much as  $\sim 40$  percent higher than theoretical ranges (Fig. 13).

In further measurements by the Copenhagen group (SIDENIUS, private communication), other examples of isotope effects were obtained for 50 keV ions. Thus, for Na<sup>24</sup> in hydrogen and deuterium ( $\epsilon = 2.4$  and 4.65) one found  $(R_D - R_H)_{exp} = +0.157$  mm, while  $(R_D - R_H)_{th} = +0.104$  mm, the ranges themselves being of order of 0.9–1.0 mm, and  $\sim 50$  percent larger than theoretical ranges. For Au<sup>198</sup> ions in hydrogen and deuterium,  $\epsilon$  is so small ( $\epsilon = 0.024$  and 0.047) that the effective power has shifted to  $s > 2$ , and  $(R_D - R_H)_{exp} = -0.061$  mm, while  $(R_D - R_H)_{th} = -0.087$  mm; experimental ranges are  $\sim 0.4$  mm, i. e. about 30 percent larger than theoretical ranges. Finally, for Ga<sup>66</sup> in helium isotope gases ( $\epsilon \sim 0.4$ ) one found  $(R_{He^4} - R_{He^3})_{exp} = -0.016$  mm, to be compared with  $(R_{He^4} - R_{He^3})_{th} = -0.006$  mm; experimental ranges are  $\sim 0.4$  mm, or 20 percent above theoretical ranges. All ranges quoted here are in mm at 300° K, 760 mm Hg. The agreement with theoretical isotope shifts of ranges is thus fairly good, and it is interesting that normally the change from larger to shorter range in the heavier isotope occurs at  $\epsilon \sim 1$ .

### Acknowledgments

A few of the above results were obtained seven years ago, following discussions with Dr. R. B. LEACHMAN on his observations of range distributions. They have been referred to various times in the literature. A brief summary of the present work (LINDHARD and SCHARFF (1961)) was published at the time of MORTEN SCHARFF's death.

We are much indebted to Drs. R. B. LEACHMANN, J. M. ALEXANDER, B. G. HARVEY, N. O. LASSEN, N. O. ROY POULSEN, W. WHALING, J. A. DAVIES, H. E. DUCKWORTH, Mr. G. SIDENIUS and many others for discussions and communication of experimental results prior to publication.

We wish to express our gratitude to all who have encouraged us and assisted in this work, in particular to P. V. THOMSEN, M. Sc.

We are much indebted to Miss S. TOLDI and Mrs. A. GRANDJEAN for assistance in the preparation of the paper.

Institute of Physics,  
University of Aarhus.

- M. I. GUSEVA, E. V. INOPIN & S. P. TSYTKO (1959). Depth of Penetration and Character of Distribution of Atoms Injected into Si<sup>30</sup> Isotope Targets. Sovj. Phys. JETP **9**, 1.
- B. G. HARVEY (1960). Recoil Techniques in Nuclear Reaction and Fission Studies. Ann. Rev. of Nucl. Sci. **10**, 235.
- B. G. HARVEY, P. F. DONOVAN, J. R. MORTON & E. W. VALYOCSEK (1959). Range Energy Relation for Heavy Atoms. UCRL-8618.
- B. G. HARVEY, W. H. WADE & P. F. DONOVAN (1960). Recoil Studies of Heavy Element Nuclear Reactions, II. Phys. Rev. **119**, 225.
- D. K. HOLMES & G. LEIBFRIED (1960). Radiation Induced Primary Knock-Ons in the Hard Core Approximation. J. Appl. Phys. **31**, 1046.
- D. K. HOLMES (1962). The Range of Energetic Atoms in Solids. "Radiation Damage in Solids", vol. I, IAEA, Vienna.
- F. JOLIOT (1934). Ranges of  $\alpha$ -Recoils in Cloud Chamber. J. Phys. Rad. (7), 5, 219.
- S. KATCOFF, J. A. MISKEL & C. W. STANLEY (1948). Ranges in Air and Mass Identification of Plutonium Fission Fragments. Phys. Rev. **74**, 631.
- R. B. LEACHMAN & H. W. SCHMITT (1954). Fine Structure in the Velocity Distribution of Slowed Fission Fragments. Phys. Rev. **96**, 1366.
- R. B. LEACHMAN & H. ATTERLING (1957). Nuclear Collision Stopping of Astatine Atoms. Arkiv f. Fysik **13**, 101.
- J. LINDHARD & M. SCHARFF (1961). Energy Dissipation by Ions in the keV Region. Phys. Rev. **124**, 128.
- J. LINDHARD, V. NIELSEN, M. SCHARFF & P. V. THOMSEN (1963). Integral Equations Governing Radiation Effects. Notes on Atomic Collisions, III. Mat. Fys. Medd. Dan. Vid. Selsk. **33**, no. 10.
- V. A. J. VAN LINT, R. A. SCHMITT & C. S. SUFFREDINI (1961). Range of 2–60 keV Recoil Atoms in Cu, Ag, Au. Phys. Rev. **21**, 14517.
- J. B. NIDAY (1961). Radiochemical Study of the Ranges in Metallic Uranium of the Fragments from Thermal Neutron Fission. Phys. Rev. **121**, 1471.
- K. O. NIELSEN (1956). The Range of Atomic Particles with Energies about 50 keV. "Electro-Magnetically Enriched Isotopes and Mass Spectrometry". Proc. 1955. Harwell Isotope Conf.
- L. C. NORTHCLIFFE (1963). Passage of Heavy Ions through Matter. To appear in Ann. Rev. Nucl. Sci.
- J. H. ORMROD & H. E. DUCKWORTH (1963). Stopping Cross-Sections in Carbon for Low Energy Atoms with  $Z \leq 12$ . To appear in Canad. J. Phys.
- G. R. PIERCY, F. BROWN, J. A. DAVIES & M. McCARGO (1963). An Experimental Study of a Crystalline Structure on the Ranges of Heavy Ions. Phys. Rev. Letters **10**, 399.
- N. T. PORILE & N. SUGARMAN (1957). Recoil Studies of High-Energy Fission of Bi and Ta. Phys. Rev. **107**, 1410.
- A. M. POSKANZER (1963). Range of 1–3 MeV Ne<sup>22</sup> Ions in Al and the Analysis of Some Na<sup>24</sup> Recoil Data. Phys. Rev. **129**, 385.
- D. POWERS & W. WHALING (1962). Range of Heavy Ions in Solids. Phys. Rev. **126**, 61.
- M. T. ROBINSON, D. K. HOLMES & O. S. OEN (1961). Monte Carlo Calculation of the Ranges of Energetic Atoms in Solids. ORNL-3212.

## References

- J. M. ALEXANDER & M. F. GAZDIK (1960). Recoil Properties of Fission Products. Phys. Rev. **120**, 874.
- J. M. ALEXANDER & D. H. SISSON (1962). Recoil Range Evidence for the Compound-Nucleus Mechanism in Reaction between Complex Nuclei. UCRL-10098.
- S. K. ALLISON & C. S. LITTLEJOHN (1957). Stopping Power of Various Gases for Li Ions of 100–450 keV Kinetic Energy. Phys. Rev. **104**, 959.
- D. L. BAULCH & J. F. DUNCAN (1957). The Range-Energy-Relation for  $\alpha$ -Recoil Atoms. Austral. J. Chem. **10**, 112.
- N. BOHR (1948). Penetration of Atomic Particles through Matter. Mat. Fys. Medd. Dan. Vid. Selsk. **18**, no. 8.
- L. BRYDE, N. O. LASSEN & N. O. ROY POULSEN (1962). Ranges of Recoil Ions from  $\alpha$ -Reactions. Mat. Fys. Medd. Dan. Vid. Selsk. **33**, no. 8.
- J. K. BØGGILD, O. H. ARRØE & T. SIGURGEIRSSON (1947). Cloud-Chamber Studies of Electronic and Nuclear Stopping of Fission Fragments in Different Gases. Phys. Rev. **71**, 281.
- H. G. CLERC, H. WÄFFLER & F. BERTHOLD (1961). Reichweite von Li<sup>8</sup>-Ionen der Energie 40–450 keV in H<sub>2</sub>, D<sub>2</sub> und He. Zeitsch. f. Naturf. **16a**, 149.
- J. A. DAVIES, J. D. MCINTYRE, R. L. CUSHING & M. LOUNSBURY (1960). The Range of Alkali Metal Ions of Kiloelectron Volt Energies in Al. Can. J. Chem. **38**, 1535.
- J. A. DAVIES & G. A. SIMS (1961). The Range of Na<sup>24</sup> Ions of Kiloelectron Volt Energies in Al. Can. J. Chem. **39**, 601.
- J. A. DAVIES, J. D. MCINTYRE & G. A. SIMS (1961). Isotope Effects in Heavy Ion Range Studies. Can. J. Chem. **39**, 611.
- B. DOMEIJ, I. BERGSTROM, J. A. DAVIES & J. UHLER (1963). A Method of Determining Heavy Ion Ranges by Analysis of  $\alpha$ -Line Shapes. To appear in Arkiv f. Fysik.
- E. M. DOUTHET & D. H. TEMPLETON (1954). The Ranges of Fragments from High Energy Fission of Uranium. Phys. Rev. **94**, 128.
- A. ERDÉLYI, W. MAGNUS, F. OBERHETTINGER & F. G. TRICOMI (1953). Higher Transcendental Functions, I. McGraw-Hill.
- U. FANO (1953). Degradation and Range Straggling of High Energy Radiations. Phys. Rev. **92**, 328.
- C. B. FULMER (1957). Scintillation Response of CsI(Tl) Crystals to Fission Fragments and Energy vs. Range in Various Materials for Light and Heavy Fission Fragments. Phys. Rev. **108**, 1113.
- W. M. GOOD & E. O. WOLLAN (1956). Range and Range Dispersion of Specific Fission Fragments. Phys. Rev. **101**, 249.

- R. A. SCHMITT & R. A. SHARP (1958). Measurement of the Range of Recoil Atoms. Phys. Rev. Letters **1**, 12.
- F. SEITZ (1949). On the Disordering of Solids by Action of Fast Massive Particles. Disc. Far. Soc. **5**, 271.
- E. R. SMITH & P. W. FRANK (1959). Recoil Range of Fission Fragments in Zirconium. WAPD-TM-198.
- F. SUZOR (1949). Tracks in Various Materials of Uranium Fission Fragments. Ann. Phys. **4**, 269.
- YA. A. TEPLOVA, V. S. NIKOLAEV, I. S. DMITRIEV and L. N. FATEEVA (1962). Slowing Down of Multicharged Ions in Solids and Gases. Sovj. Phys. JETP **15**, 31.
- E. W. VALYOCSEK (1959). Range and Range Straggling of Heavy Recoil Atoms. UCRL-8855.
- W. WHALING (1958). The Energy Loss of Charged Particles in Matter. Hdb. d. Phys. vol. **34**, 193.
- A. VAN WIJNGAARDEN & H. E. DUCKWORTH (1962). Energy Loss in Condensed Matter of  $H^1$  and  $He^4$  in the Energy Range 4 to 30 keV. Can. J. Phys. **40**, 1749.
- L. WINSBERG & J. M. ALEXANDER (1961). Ranges and Range Straggling of  $Tb^{149}$ , At and Po. Phys. Rev. **121**, 518.